อนุภาคควอเทอร์ไนซ์ไคโทซานที่ติดฉลากเรืองแสงเตรียมโดยการประกอบตัวเองของแอมฟิฟิลิกไคโทซาน

นางสาวกัญญา ตะบูนพงศ์

วิทยานิพนธ์นี้เป็นส่วนหนึ่งของการศึกษาตามหลักสูตรปริญญาวิทยาศาสตรมหาบัณฑิต
สาขาวิชาปิโตรเคมีและวิทยาศาสตร์พอลิเมอร์
คณะวิทยาศาสตร์ จุฬาลงกรณ์มหาวิทยาลัย
ปีการศึกษา 2554

FLUORESCENT-LABELED QUATERNIZED CHITOSAN PARTICLES PREPARED BY SELF-ASSEMBLY OF AMPHIPHILIC CHITOSAN

Miss Kanya Taboonpong

A Thesis Submitted in Partial Fulfillment of the Requirements
for the Degree of Master of Science Program in Petrochemistry and Polymer Science
Faculty of Science
Chulalongkorn University
Academic Year 2011

Thesis Title	FLUORESCENT-LABELED QUATERNIZED CHITOSAN PARTICLES PREPARED BY SELF-ASSEMBLY OF AMPHIPHILIC CHITOSAN
By	Miss Kanya Taboonpong
Field of Study	Petrochemistry and Polymer Science
Thesis Advisor	Associate Professor Voravee P. Hoven, Ph.D.

Accepted by the Faculty of Science, Chulalongkorn University in Partial Fulfillment of the Requirements for the Master's Degree

……Dean of the Faculty of Science
(Professor Supot Hannongbua, Dr.rer.nat.)

THESIS COMMITTEE

……Chairman
(Associate Professor Supawan Tantayanon, Ph.D.)

……Thesis Advisor
(Associate Professor Voravee P. Hoven, Ph.D.)

……Examiner
(Associate Professor Nuanphun Chantarasiri, Ph.D.)

……External Examiner
(Associate Professor Metha Rutnakornpituk, Ph.D.)

กัญญา ตะบูนพงศ์:อนุภาคควอเทอร์ไนซ์ไคโทซานที่ติดฉลากเรืองแสงเตรียมโดยการประกอบตัวเองของแอมฟิฟิลิกไคโทซาน. (FLUORESCENT-LABELED QUATERNIZED CHITOSAN PARTICLES PREPARED BY SELF-ASSEMBLY OF AMPHIPHILIC CHITOSAN) อ.ที่ปรึกษาวิทยานิพนธ์หลัก: รศ. ดร.วรวีร์ โฮเว่น, 64 หน้า.

งานวิจัยนี้ประสบความสำเร็จในการเตรียมอนุภาคแอมฟิฟิลิกไคโทซานสามชนิดจากทาโลอิลไคโทซาน อนุภาคสองชนิดแรก คือ Ph-CS-HTAP และ Ph-CS-DDAMT มีหมู่ทาโลอิลเป็นหมู่ไม่ชอบน้ำ และมีหมู่เอ็น-[(2-ไฮดรอกซิล-3-ไทรเมทิลแอมโมเนียม)]โพรพิล และหมู่เอ็น-ไดเมทิลแอมโมเนียม เมทิล]ไตรเอโซลิลเป็นหมู่ชอบน้ำ ตามลำดับ ในขณะที่อนุภาคชนิดที่สามคือ Pyr-CS-HTAP มีไพรีนซึ่งเป็นสีย้อมเรืองแสงเป็นหมู่ไม่ชอบน้ำ และ หมู่เอ็น-[(2-ไฮดรอกซิล-3-ไทรเมทิลแอมโมเนียม)]โพรพิลเป็นหมู่ชอบน้ำ พิสูจน์ยืนยันโครงสร้างทางเคมีของอนุพันธ์แอมฟิฟิลิกไคโทซานด้วยโปรตอนเอ็นเอ็มอาร์และเอฟที-ไออาร์สเปกโทรสโกปี อนุภาคชนิด Ph-CS-HTAP และ Pyr-CS-HTAP แสดงประจุเป็นบวกและมีขนาดอยู่ในระดับไมโครเมตร ในขณะที่อนุภาคชนิด Ph-CS-DDAMT แสดงประจุเป็นลบและมีขนาดเล็กกว่ามาก อนุภาคชนิด Pyr-CS-HTAP มีสัณฐานวิทยาน่าสนใจ โดยมีลักษณะคล้ายผลแบล๊คเบอร์รี่ โครงสร้างและสมบัติการเรืองแสงไม่ว่องไวต่อการเปลี่ยนแปลงพีเอชและอุณหภูมิ อนุภาคเกิดการแตกออกเมื่อสัมผัสกับเฮกเซน แต่จะได้อนุภาคกลับคืนมาหลังจากการกำจัดเฮกเซนและแทนที่ด้วยน้ำ จากการทดลองพบว่าอนุภาคที่เตรียมได้ทั้งสามชนิดไม่แสดงฤทธิ์ในการต้านแบคทีเรีย อย่างไรก็ตามอนุภาคชนิด Pyr-CS-HTAP ไม่เป็นพิษต่อเซลล์ mouse leukaemic monocyte macrophage cell line (RAW 264.7 cells) ความสามารถในการนำเข้าสู่เซลล์และการกักเก็บไนล์เรดซึ่งเป็นแบบจำลองของสารไม่ชอบน้ำแสดงให้เห็นถึงศักยภาพในการนำอนุภาคดังกล่าวไปประยุกต์ในการปลดปล่อยแบบควบคุมและการติดตามปรากฏการณ์ทางชีวภาพ

สาขาวิชา ปิโตรเคมีและวิทยาศาสตร์พอลิเมอร์ ลายมือชื่อนิสิต .....

ปีการศึกษา 2554 ลายมือชื่ออ.ที่ปรึกษาวิทยานิพนธ์หลัก .....

5272204123 : MAJOR PETROCHEMISTRY AND POLYMER SCIENCE
KEYWORDS : CHITOSAN PARTICLES/ QUATERNIZATION/ AMPHIPHILIC CHITOSAN/ FLUORESCENT-LABELED CHITOSAN PARTICLES

KANYA TABOONPONG: FLUORESCENT-LABELED QUATERNIZED CHITOSAN PARTICLES PREPARED BY SELF-ASSEMBLY OF AMPHIPHILIC CHITOSAN. ADVISOR: ASSOC. PROF. VORAVEE P. HOVEN, Ph.D., 64 pp.

Three types of amphiphilic chitosan particles were successfully prepared from phthaloyl chitosan (PhCS). The first two types, Ph-CS-HTAP and Ph-CS-DDAMT particles had phthaloyl group as hydrophobic entity and *N*-[(2-hydroxyl-3-trimethyl ammonium)]propyl (HTAP) and 4-[(*N*-decyl-*N*,*N*-dimethylammonium methyl)]triazolyl (DDAMT) as hydrophilic entity, respectively. The third type, Pyr-CS-HTAP particles had fluorescent dye, pyrene, as hydrophobic entity and HTAP as hydrophilic entity. Chemical structures of all particles were verified by ^{1}H NMR and FT-IR spectroscopy. Ph-CS-HTAP and Pyr-CS-HTAP particles were positively charged and had a size in a micrometer range, whereas Ph-CS-DDAMT particles possessed negative charge and were much smaller in size. Interestingly, Pyr-CS-HTAP particles exhibited blackberry-like morphology. Their structure and fluorescence property were not sensitive to pH and temperature variation. They deaggregated upon the treatment with hexane, but can be recovered after hexane removal and water replacement. None of the particles possessed antibacterial activity against all bacterial strains tested. Nevertheless, Pyr-CS-HTAP particles were not toxic when tested with mouse leukaemic monocyte macrophage cell line (RAW 264.7 cells). The ability to be taken up by the cells and encapsulate nile red, a model hydrophobic molecule, suggests that these particles are potential material for controlled delivery and bioimaging applications.

Field of Study: Petrochemistry and Polymer Science Student's Signature .....
Academic Year: 2011 Advisor's Signature .....

ACKNOWLEDGEMENTS

The accomplishment of this thesis can be attributed to the extensive support from my thesis advisor, Associate Professor Dr. Voravee P. Hoven. I am grateful for her invaluable suggestion, kindness, and encouragement throughout the course of my research. I am sincerely grateful to the members of the thesis committee, Associate Professor Dr. Supawan Tantayanon, Associate Professor Dr. Nuanphun Chantarasiri and Associate Professor Dr. Metha Rutnakornpituk for reviewing my thesis and for their valuable constructive comments and suggestions. And I would like to express my gratitude to Associate Professor Dr. Tanapat Palaga of Department of Microbiology for his kind suggestion and providing facilities for biological tests and Ms. Sunatda Arayachukiat of Program of Macromolecular Science for assistance with cellular uptake study. I also thank Ms.Chonnaree Wisutsittsiwong of Department of Microbiology, for cytotoxicity tests.

This thesis would not be successful without kindness and helps from Institute of Biotechnology and Genetic Engineering, Chulalongkorn University for providing bacteria testing facilities. I gratefully acknowledge the financial support provided by Research Team Consolidation Grant, The Thailand Research Fund (RTA5280002), a research fund for Master student (Ms. Nadda Booranabunyat) from the Thailand Research Fund (MRG-WII535S006) and the Center for Petroleum, Petrochemicals and Advanced Materials, Chulalongkorn University.

Furthermore, I would like to thank all members of Organic Synthesis Research Unit (OSRU), and all my friends, for their friendliness, helpful discussions, cheerful attitude and encouragements during my thesis work. Finally, I also wish to especially thank my family members for their love, kindness and support throughout my entire study.

CONTENTS

Page

Page

Page

LIST OF TABLES

LIST OF FIGURES

Figure Page

LIST OF SCHEMES

Scheme Page

LIST OF ABBREVIATIONS

CS	: Chitosan
CLSM	: Confocal Laser Scanning Microscopy
DD	: Degree of deacetylation
DDAMT	: 4-[(*N*-decyl-*N*,*N*-dimethylammonium methyl)]triazolyl
DIEA	: *N*,*N*-diisopropyl ethylamine
DMF	: *N*,*N*-dimethylformamide
DPDABr	: *N*,*N*-dimethyl-*N*-prop-2-yn-1-yldecan-1-ammonium bromide
DS	: Degree of substitution
FT-IR	: Fourier transform infrared spectroscopy
GTMAC	: Glycidyltrimethylammonium chloride
HTAP	: *N*-[(2-hydroxyl-3- trimethylammonium)]propyl
NMR	: Nuclear magnetic resonance spectroscopy
NMR	: Nuclear magnetic resonance spectroscopy
N_3-PhCS	: Azide-functionalized phthaloylchitosan
PCS	: Photon correlation spectroscopy
PhA	: Phthalic anhydride
PhCS	: Phthaloylchitosan
Ph-CS-DDAMT	: Phthaloylchitosan grafted with 4-[(*N*-decyl-*N*,*N*-dimethylammonium methyl)]triazolyl
Ph-CS-HTAP	: Phthaloylchitosan grafted with *N*-[(2-hydroxyl-3-trimethylammonium)]propyl
Pyr-PhCS	: Pyrene-functionalized phthaloylchitosan
Pyr-CS-HTAP	: Pyrene-functionalized chitosan grafted with *N*-[(2-hydroxyl-3- trimethylammonium)]propyl
SEM	: Scanning electron microscopy
TEM	: Transmission electron microscopy
ζ-potential	: Zeta-potential

CHAPTER I
INTRODUCTION

1.1 Statement of Problem

Chitosan is a natural, non-toxic, and biodegradable biopolymer that exhibits antibacterial activity only in acidic media of which amino groups in its structure are protonated (above pKa of 6.5). In order to increase the antibacterial activity of chitosan over a broader pH range, quaternization has been successfully employed to convert amino groups to permanent positively charged quaternary groups. Recently, it has also been demonstrated that chitosan in the form of nanoparticles exerted a higher antibacterial activity against a number of bacterial strains than chitosan solution. It was proposed that the greater surface area of the particles is responsible for such superior antibacterial action. Therefore, it is anticipated that quaternized chitosan in the form of particles would exhibit greater ability in suppressing bacterial growth when compared with chitosan particles or quaternized chitosan solution.

Self-assembly is well recognized as a versatile technique for inducing particle formation from amphiphilic polymer having both hydrophobic and hydrophilic entities. In particular, the method has been successfully employed to generate particles from amphiphilic chitosan having phthaloyl as hydrophobic entity and mPEG as hydrophilic entity. The particles with a controllable size range possess a great potential as drug carriers.

Fluorescent labeling has been known as an effective tool to monitor substance uptake by biological systems. In the case of particles, the fluorescent dye can be either chemically tagged to or physically encapsulated in the particles. Previously, it has been demonstrated that antibacterial activity of fluorescein isothiocyanate-labeled oleoyl-chitosan nanoparticles against *S. aureus* and *E. coli* can be assessed by fluorescence microscopy.

Here in this research, we are interested in preparing quaternized chitosan particles that may be used to monitor antibacterial mechanism via fluorescence techniques which cannot be realized by conventional antibacterial assays based on optical density measurements, viable counts, or clear zone determination. Taking

advantage of pyrene being a hydrophobic fluorescent dye, fluorescent-labeled quaternized chitosan particles can be conveniently prepared by self-assembly of amphiphilic chitosan having pyrene as a hydrophobic entity and *N*-[(2-hydroxyl-3-trimethylammonium)] propyl (HTAP) as a hydrophilic entity which were attached to chitosan backbone at C-2 hydroxyl and amino position, respectively. Huisgen's 1,3-dipolar cycloaddition was particularly selected as a route to link pyrene to chitosan since the reaction can be performed under mild condition with short reaction time and leads to selectively high yield.

The fluorescent-labeled quaternized chitosan particles were characterized by several techniques, namely Fourier transformed infrared spectroscopy (FT-IR), nuclear magnetic resonance spectroscopy (^{1}H NMR), photon correlation spectroscopy (PCS), scanning electron microscopy (SEM), transmission electron microscopy (TEM), and fluorescence spectrophotometry. Effects of solvent, temperature, and pH on the stability of the particles were determined.

Antibacterial activity against a Gram-positive bacteria, ***Staphylococcus aureus (S.aureus)***, and a Gram-negative bacteria, ***Escherichia coli (E.coli)***, fluorescent-tagged ***Escherichia coli HB101 pGLO***, were performed by viable cell counting methods. Fluorescence and confocal microscopy were used to monitor the interactions between bacteria and the particles. Cytotoxicity and cellular uptake of fluorescent-labeled quaternized chitosan particles were also evaluated.

1.2 Objectives

1.2.1 To prepare and characterize fluorescent-labeled quaternized chitosan particles formed by self assembly of amphiphilic chitosan

1.2.2 To determine its ability to be used for monitoring antibacterial activity

1.3 Scope of the Investigation

1.3.1 Synthesis and characterization of amphiphilic chitosan

1.3.2 Preparation and characterization of fluorescent-labeled quaternized chitosan particles formed by self-assembly of amphiphilic chitosan

1.3.3 Determination of antibacterial activity of the particles

1.3.4 Monitoring interactions between bacteria and the particles using fluorescence techniques

1.3.5 Evaluation of cytotoxicity and cellular uptake of the particles

CHAPTER II
THEORY AND LITERATURE REVIEW

2.1 Chitosan

Chitosan is a partially deacetylated form of chitin, found in the exoskeleton of insect, shell of crustaceans and fungal cell walls. A common method for the synthesis of chitosan is the deacetylation of chitin using sodium hydroxide in excess as a reagent and water as a solvent (Scheme 2.1). The degree of deacetylation (%DD) in commercial chitosan is usually in a range of 60-100 %.

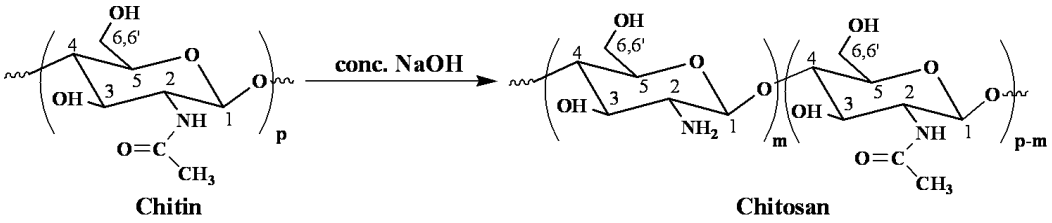

Scheme 2.1 Structures of chitin and chitosan

Chitosan is a linear polysaccharide composed of randomly distributed *β*-(1-4)-linked *D*-glucosamine (deacetylated unit) and *N*-acetyl-*D*-glucosamine (acetylated unit). The solubility of chitin is remarkably poorer than that of cellulose, because of the high crystallinity of chitin, supported by hydrogen bonds mainly through the acetamido group.[1] The amino group in chitosan has a pKa value of ~6.5, which leads to a protonation in acidic to neutral solution, chitosan can be soluble in acidic media with a charge density being dependent on pH and %DD. Chitosan has abundant hydroxyl groups (at C-6 and C-3) and highly reactive amino group (at C-2). These functional groups are readily available for a variety of functionalization. Due to a number of favorable characteristics of chitosan such as biocompatibity, biodegradability, low toxicity and antibacterial activity, chitosan is used in many applications such as medicine, cosmetics, food industry and agriculture. [2,3]

2.2 Quaternary Ammonium-containing Chitosan Derivatives and Their Antibacterial Activities

The fact that chitosan can only be soluble in acidic media has, to some extent, limited its usage in some specific applications, especially those are sensitive to acidic pH. For this reason, a number of chemical modification strategies have been continuously introduced in order to improve its solubility in a broader pH range. One common approach is to introduce pH-independent, positively charged quaternary ammonium groups to chitosan structure. The work in this area was pioneered by Domard *et al.* in 1986 [4] on the synthesis of *N,N,N*-trimethyl chitosan chloride (TMC) by methylation of chitosan having high %DD using methyl iodide in the presence of sodium hydroxide.

Among all derivatives having antibacterial activity, namely carboxyalkylated chitosan [5,6,7], sulfonated chitosan [8], ethylamine hydroxyethyl chitosan [7], guanidinylated chitosan [9] and oleyl chitosan [10], quaternized chitosan has attracted most attention. Having permanent positive charges, the quaternized derivative should, in principle, favorably interact with negatively charged membrane of bacteria. The hydrophobicity of the alkyl groups incorporated via quaternization should somewhat impart antibacterial action on some bacterial strains of which membranes are dominantly covered with lipid-like layer.

In 1997, Kim *et al.* [11] synthesized *N*-alkyl chitosan derivatives by introducing methyl, butyl, octyl and dodecyl groups to the amine groups of chitosan via Schiff's base intermediates followed by quatemization using methyl iodide to produce water soluble cationic polyelectrolytes. These *N*-alkyl chitosan derivatives exhibited antibacterial activities against *Staphylococcus aureus (S.aureus)*. The antibacterial activities of the chitosan derivatives with quaternary ammonium salt had a direct relationship with the chain length of the alkyl substituent, and this increased activity could be explained as a result of elevating hydrophobicity of the derivatives.

In 2000, Seong, *et al.* [12] used glycidyltrimethyl ammonium chloride (GTMAC) as a quaternizing agent. The product which is called *N*-[(2-hydroxyl-3-trimethylammonium)propyl] chitosan chloride (HTACC) can be prepared by ring opening of GTMAC by amino groups of chitosan (Scheme 2.2). The HTACC shows

excellent solubility in water and great antimicrobial activity when treated on cotton fabric. The activity was still maintained even after repetitive washing for 50 times.

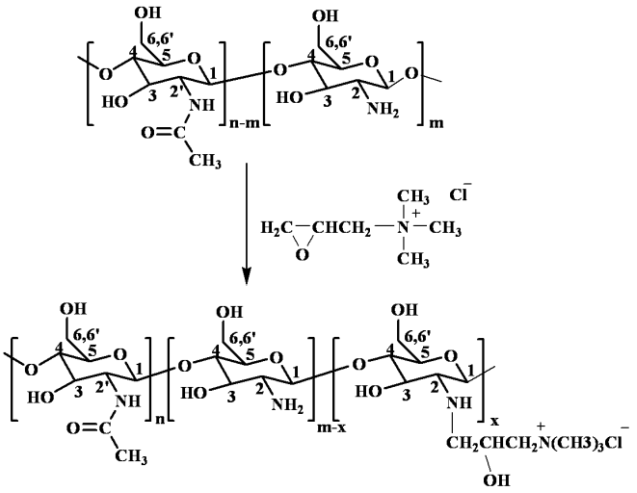

Scheme 2.2 Synthesis of *N*-[(2-hydroxyl-3-trimethylammonium)propyl] chitosan chloride (HTACC)

In 2001, Jia *et al.* [13] prepared different quaternized chitosan derivatives which are *N,N,N*-trimethyl chitosan, *N*-propyl-*N,N*-methyl chitosan, and *N*-furfuryl-*N,N*-dimethyl chitosan. These derivatives can be synthesized by the reaction between amino groups of chitosan and aldehydes to form Schiff base intermediates, followed by quaternization with methyl iodide (Scheme 2.3). All derivatives were not only soluble in water but also expressed a better antibacterial activity against *Escherichia coli* (*E. coli*) than native chitosan. The activity also depends upon its molecular weight as well as the concentration of acetic acid used for solubilization.

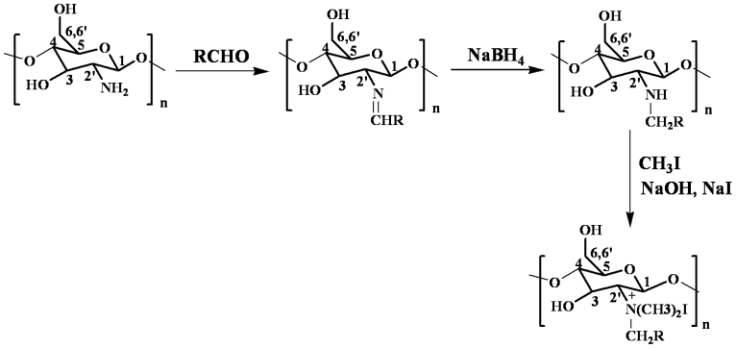

Scheme 2.3 Synthesis of quaternized *N*-alkyl chitosan

In 2004, Avadi *et al.* [14] prepared *N*-diethylmethyl chitosan (DEMC) by *N*-reductive alkylation with formaldehyde and followed by quaternization with ethyl iodide in the presence of sodium iodide. The antibacterial activity of DEMC was found to be superior to the original chitosan.

In 2008, Sajomsang *et al.* [15] reported the synthesis of *N*-arylated chitosan via Schiff base formation using aromatic aldehyde which was later reduced by sodium cyanoborohydride followed by methylation using iodomethane under basic condition and finally yielded methylated *N*-alkylated chitosan (Scheme 2.4). The total degree of quaternization of chitosan derivatives depends on the extent of N-substitution and the sodium hydroxide concentration in methylation step. The antibacterial activity of the derivatives was tested against *E.coli* and *S.aureus*. Minimum inhibitory concentrations (MIC) of these derivatives ranged from 32 to128 µg/mL.

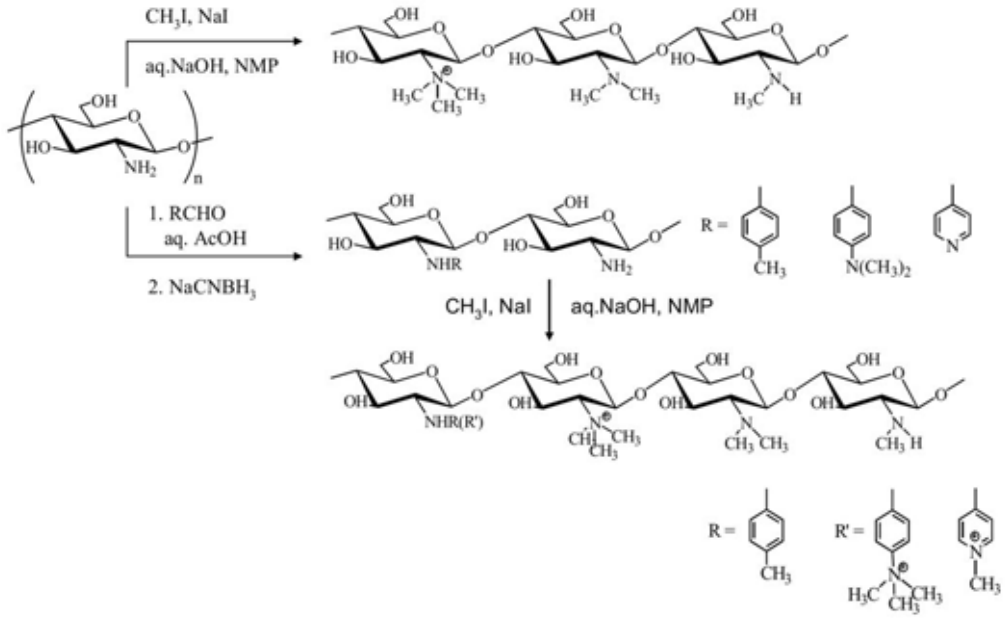

Scheme 2.4 Synthesis of methylated chitosan and *N*-aryl chitosan [15]

In 2009, Sajomsang *et al.* [16] also used a two- step reaction, the reductive alkylation and methylation, to synthesize methylated *N*-(4-*N,N*-dimethylaminocinnamyl) chitosan chloride (MDMCMCh), methylated *N*-(4-pyridylmethyl) chitosan chloride (MPyMeCh), and *N,N,N*-trimethyl chitosan chloride

(TMChC) (Scheme 2.5). The results of antibacterial activity against *E.coli* ATCC 25922 (Gram-negative) and *S.aureus* ATCC 6538 (Gram-positive) of all derivatives revealed that the MDMCMCh exhibited greater antibacterial activity than TMChC whereas MPyMeCh exhibited reduced antibacterial activity against both bacteria.

In 2012, Liu *et al.* [17] prepared *O*-(3,6-hydroxyethyl) chitosan (HC) by using chlorohydrins as a grafting agent on to *N*-(2-phthaloyl) chitosan and followed by reduction with hydrazine hydrate. The antibacterial activity of HC against *Enterococcus* and *E. coli* was found to be much better than chitosan owing to the enhanced degree of protonation. In the same year, Yin *et al.* [18] synthesized seven Schiff bases from *O*-carboxymethyl chitosan (CMC) (obtained after deacetylation and carboxymethylation of chitosan) and *para*-substituted benzaldehydes, (Scheme 2.6). Antibacterial activity of the Schiff bases against *E.coli* and *S. aureus* were varied with the substituents at the *para* position of benzaldehyde, and decreased according to the following sequence: $OCH_3 > CH_3 > H > F > Cl > Br > NO_2$. It could be concluded that electron-donating group at the *para* position of benzaldehyde increases the antibacterial activity of the chitosan Schiff bases. The outcome is opposite for electron-withdrawing group.

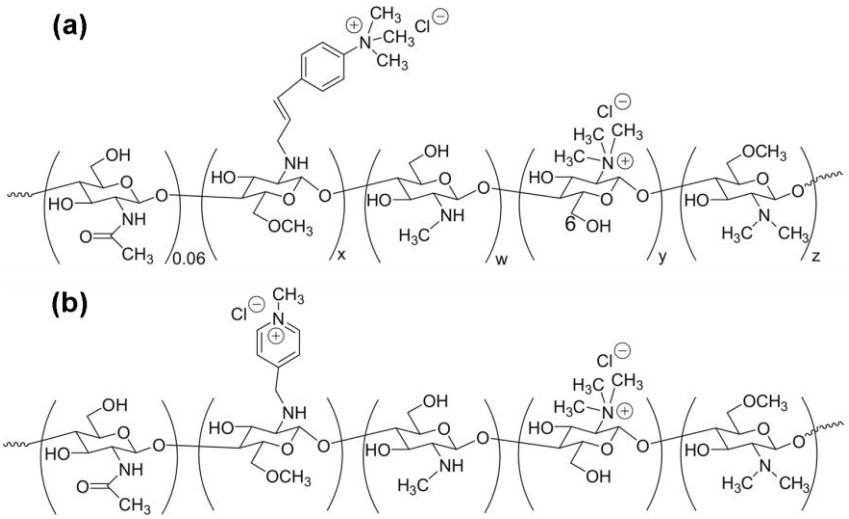

Scheme 2.5 Structure of (a) methylated *N*-(4-*N,N*-dimethylaminocinnamyl) chitosan chloride (MDMCMCh) and (b) methylated *N*-(4-pyridylmethyl) chitosan chloride (MPyMeCh) [16]

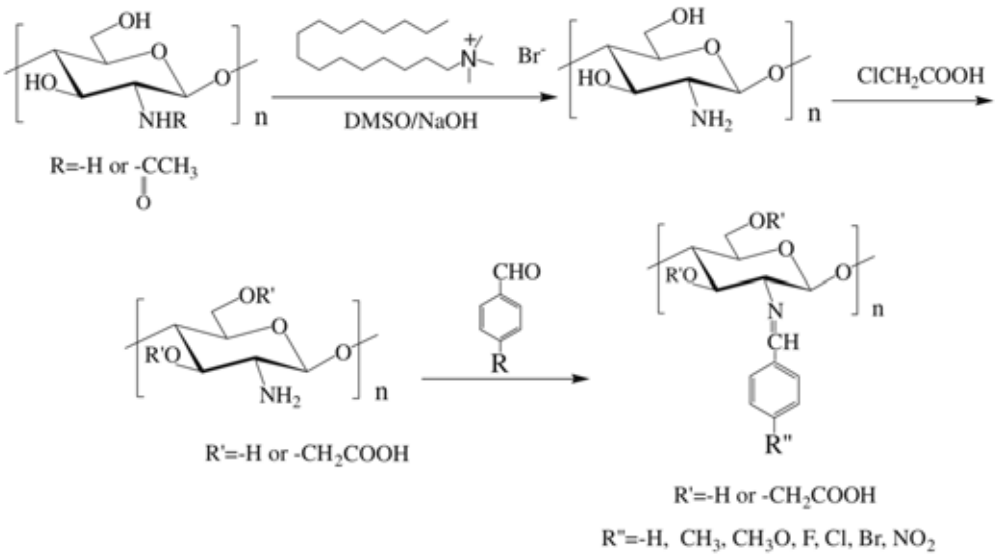

Scheme 2.6 Synthesis of Schiff base chitosan [18]

Using a well-established quaternization route based on a two-step process: reductive *N*-alkylation followed by methylation, Vallapa *et al.* [19] recently demonstrated that quaternary ammonium entities can be successfully introduced to the surface of pre-fabricated chitosan films by performing the reactions under heterogeneous conditions. The process can truly be simplified in the absence of tedious purification step that are certainly required if the quaternization is done homogeneously in solution. The superior antibacterial activity of the surface-quaternized chitosan film against *S. aureus* and *E. coli*, to that of the virgin chitosan film at neutral pH was verified by viable cell count method and observation of damaged bacterial morphology by SEM (Figure 2.1).

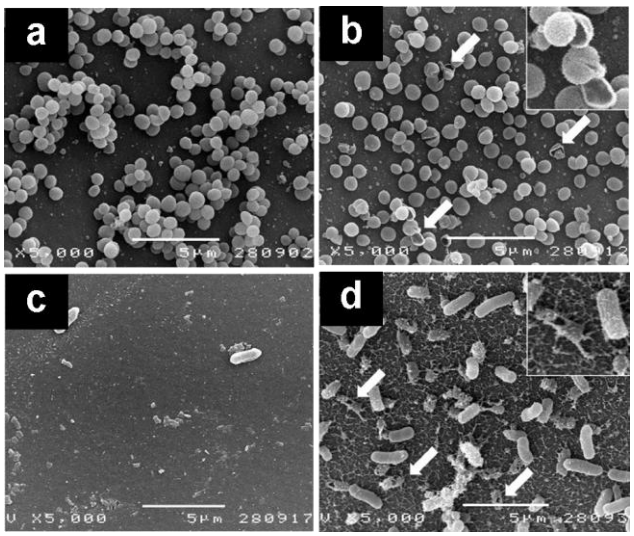

Figure 2.1 SEM micrographs of the (a,c) chitosan and (b,d) quaternized *N*-benzyl chitosan films with 1.2 M of CH_3I after being incubated with the suspension of *S. aureus* and *E. coli* (OD_{600}=0.5) for 24 h, respectively. [19]

Effective antibacterial efficacy of chitosan particles has been recently recognized and reported. In 2004, Qi and co-workers [20] reported that chitosan nanoparticles expressed a higher antibacterial activity against a number of bacterial strains, namely *E. coli, Salmonella choleraesis, S. typhimurium and S. aureus* than chitosan solution. It is believed that the greater surface area of the particles provided a more intimate contact with the surface of bacterial cells. In 2006, Ye and co-workers [21], have shown that cotton fabrics coated with core-shell particles, having poly(*n*-butyl acrylate) as the core and chitosan as the shell, showed an excellent antibacterial activity against *S. aureus* with a reduction in viable bacteria numbers of more than 99%. Particles fabricated from chitosan formerly quaternized by hexyl bromide and incorporated in poly(methyl methacrylate) bone cement were found to be effective antibacterial fillers against *S. aureus* and *S. epidermidis* under a neutral pH environment as reported by Shi *et al.* in 2006 [22].

Incorporation of metal ion was reported as an alternative way to enhance antibacterial activity to chitosan particles. Qi and co-workers [20] have suggested that the antibacterial activity against *E. coli* K88 was significantly enhanced by incorporating Cu^{2+} into chitosan particles [23] (Figure 2.2). Later, Du *et al.* [24] showed that chitosan particles loaded with various metal ions, such as Ag^{+}, Cu^{2+}, Zn^{2+},

Mn^{2+} or Fe^{2+}, exhibited a higher antibacterial effect against *E. coli*, *S. choleraesuis* and *S. aureus* than that of unmodified chitosan particles. In the following year, Du *et al.* [25] Moreover, it was found that antibacterial activity was directly proportional to the charge density of particles expressed in term of zeta potential.

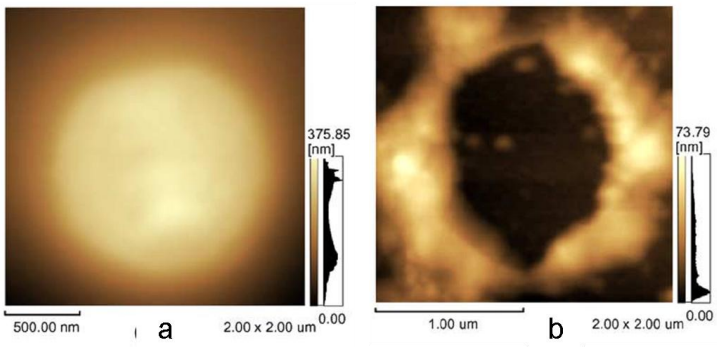

Figure 2.2 Atomic force micrographs (AFMs) of *S. choleraesuis* cells after treatment with chitosan nanoparticles suspension for different times. (a) Nontreated cells and (b) treated cells for 2 h [20].

In 2012, Wiarachai *et al.* [26] revealed that the same heterogenous quaternization based on a two-step process: reductive *N*-alkylation followed by methylation, earlier employed by Vallapa *et al.* [19] and direct methylation can be used to generate surface-quaternized chitosan particles with a ζ-potential ranging from +23.2 to +46.8 mV. Results from viable cell counts suggested that all quaternized chitosan particles exhibited superior antibacterial activity against *S. aureus*, as compared to the native chitosan particles at neutral pH. Only some quaternized chitosan particles, especially those having a high charge density and bearing large alkyl substituent groups, were capable of suppressing the growth of *E. coli* (Figure 2.3). The inhibitory efficiency of the quaternized chitosan particles was quantified in terms of the minimum inhibitory concentration (MIC).

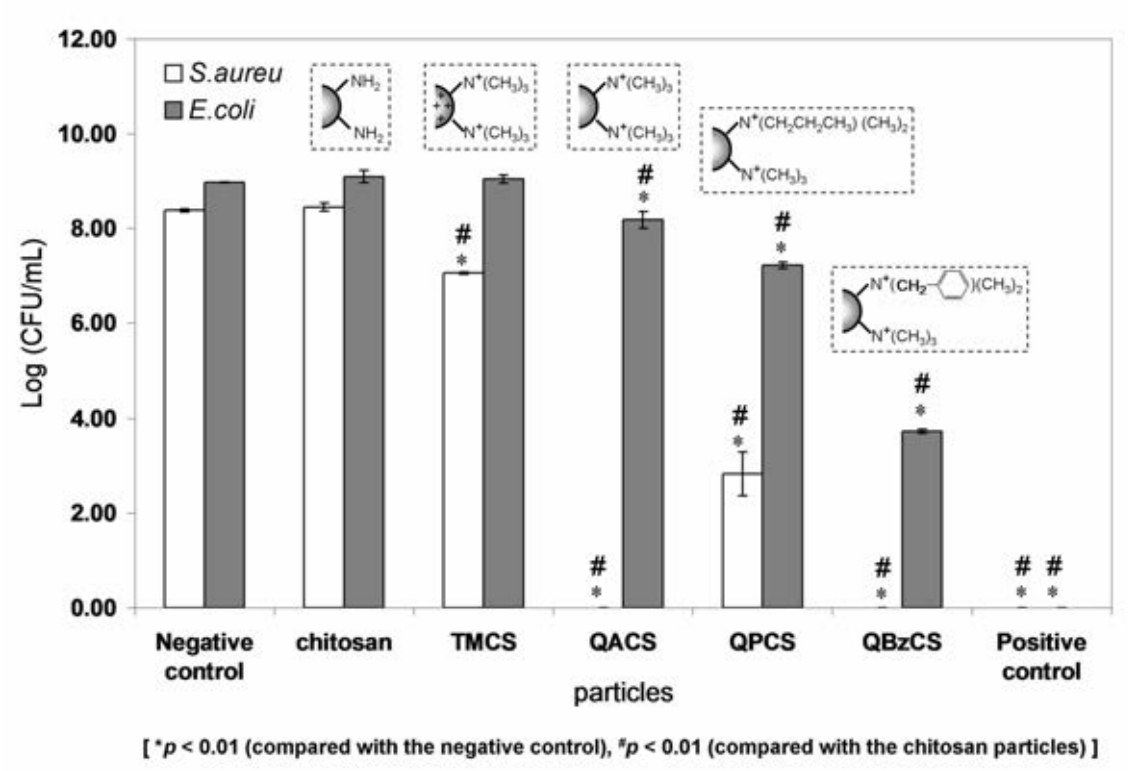

Figure 2.3 Antibacterial efficacy of quaternized chitosan particles against the representative Gram-positive (*S. aureus*) and Gram-negative (*E. coli*) bacteria expressed in term of the total number of replication competent cells in log(CFU/mL) [26].

2.3 Self-assembly of Amphiphilic Chitosan

Self-assembly process can be defined as spontaneous and reversible organization of molecular units into ordered structures by non-covalent interactions. This technique allows particles to be formed from amphiphilic polymers having both hydrophobic and hydrophilic entities. In principle, the hydrophobic parts should form the inner core and the hydrophilic parts should situate outside as corona in polar solvent. The organization would be opposite in non-polar solvent**.** This technique should afford particles in high yield with controllable dimension. Therefore, it is known as an effective tool for the preparation of nanoparticles as carriers for active ingredients such as drugs or vitamin which can be used in medical, pharmaceutical or cosmetic applications. There are many research works on the preparation of chitosan particles by self-assembly of amphiphilic chitosan.

Yoksan *et al*. [27] and Choochottiros *et al*. [28] synthesized *N*-phthaloylchitosan grafted with poly(ethylene glycol) methyl ether (mPEG) and studied the colloidal phenomena and nanosphere formation as a function of solvent and pH (Scheme 2.7). The mPEG (Mn = 5,000) gave spheres with sizes about 80–100 nm, whereas mPEG (Mn = 550) provided spheres with an average size of 400–500 nm. As demonstrated by Opanasopit *et al*. [29], the particles can act as a carrier for camptothecin (CPT) of which its release depends upon %DD (80, 85, 90 and 95%). A sustained release profile was obtained at high %DD.

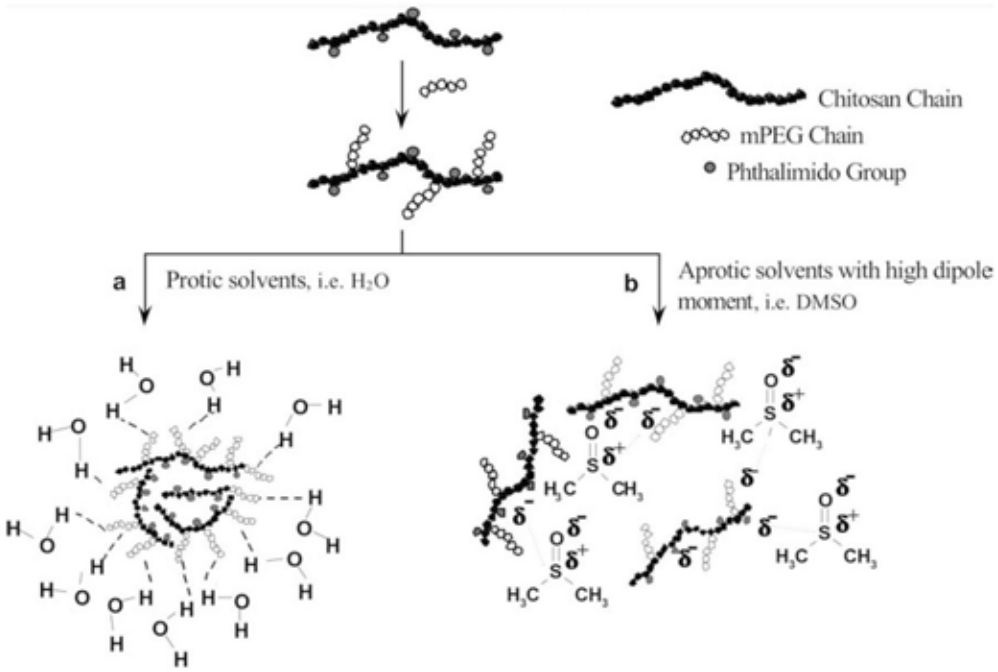

Scheme 2.7 Formation of *N*-phthaloylchitosan grafted with poly(ethylene glycol) methyl ether (mPEG) in protic and aprotic solvents [27].

In 2005, Kim *et al*. [30] prepared deoxycholic acid modified glycol chitosan self-aggregates by covalent attachment of deoxycholic acid to glycol chitosan (GCD). The mean sizes of self-aggregates were in a range of 245-450 nm, depending on %DD. The critical aggregation concentration (CAC) values of the GCD conjugates decreased with the increasing hydrophobic deoxycholic acid and varied in a range of 0.038-0.260 mg/mL. The GCD of which degree of substitution was 30% maintained its self-aggregate structure in physiological conditions and stable for up to 10 days.

In 2008, Anumansirikul *et al*. [31] synthesized methyl ether terminated poly(ethylene) glycol)-4-methoxy cinnamoyl phthaloylchitosan (PCPLC) and methyl ether terminated poly(ethylene glycol) phthaloylchitosan (PPLC). Then the formation of particles by self-assembly and 2-ethylhexyl-4-methoxy cinnamate (EHMC) encapsulation of the particles were investigated. It was found that minimal *E* to *Z* photoisomerization was observed when EHMC was encapsulated in PCPLC particles. The results indicated that the grafted UVB absorptive chromophore, 4-methoxycinnamoyl moieties, situated at the shell of PCPLC helped protecting EHMC from photoisomerization.

In 2009, Liu *et al*. [32] synthesized amphiphilic chitosan grafted with polycaprolactone (PCL) and poly(ethylene glycol) methyl ether which act as hydrophobic and hydrophilic entity, respectively. The reaction was carried out by reacting phthaloyl-protected chitosan with functional PCL-COOH and mPEG-COOH. Nanosized particles were formed upon dialysis in water as verified by dynamic light scattering and transmission electron microscopy. The particles could form in acidic solution and became less stable with increasing the solution pH.

In 2009, Ngawhirunpat *et al*. [33] incorporated camptothecin (CPT) in a polymeric micelle prepared from cholic acid chitosan grafted poly(ethylene glycol)methyl ether (CS-mPEG-CA). Among three incorporation methods (dialysis, emulsion and evaporation methods), an emulsion method showed the highest CPT incorporation efficiency. The mean particle sizes were increased from 93-120 nm to 150-390 nm upon CPT loading.

In 2009, Xing *et al.* [34] prepared oleoyl-chitosan nanoparticles tagged with fluorescein isothiocyanate (FITC-OCSNP). As monitored by fluorescence microscopy, it was found that the FITC-OCSNP firstly attached to the membrane of *E. coli* cells and then penetrated into the cells after a certain period of time leading to the dead of *E. coli*. In contrast, the FITC-OCSNP can promptly penetrate through the membrane of *S. aureus* and consequently causes the cell breakage.

2.4 Bacteria [35]

Bacteria are prokaryotic microorganisms normally found in nature. Bacteria have a wide range of shape, for example sphere and rod. Bacteria can be divided into two groups by the Gram staining technique. The stains of bacteria are separated by the attraction of different dyes onto the bacterial cell wall. It should be noted that the gram positive and gram negative do not indicate the charge of cell. The different results in Gram staining are owing to difference in structure of the cell wall and how it reacts to the series of reagents applied to the cells.

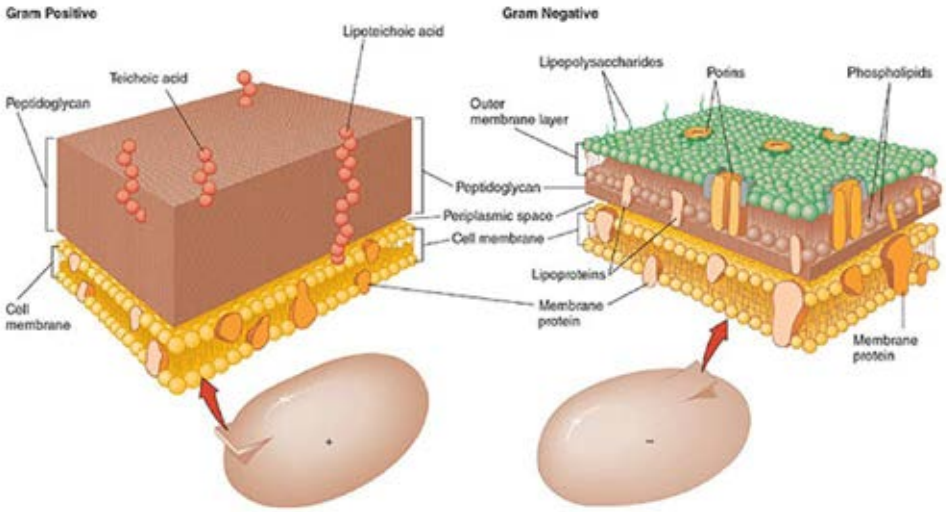

Figure 2.4 Structure of gram positive and gram negative cell walls [35]

Gram positive bacteria have a thick cell wall consisting of peptidoglycan layer ranging from 20 to 80 nm in thickness. It also contains polysaccharides, including teichoic acid and lipoteichoic acid (Figure 2.4). Teichoic acid is a polymer of ribitol or glycerol and phosphate embedded in the peptidoglycan layer. Lipoteichoic acid is attached to the lipids in the plasma membrane. There is a thin periplasmic space between the cell membrane and cell wall but in some case, the cell wall of gram positive bacteria are very close to the cell membrane.

In the case of gram negative bacteria, the cell wall has a thinner layer of peptidoglycan compared to gram positive bacteria and has a space surrounding peptidoglycan layer but it also contains an outer membrane layer (Figure 2.4). The

outer membrane consists of special type of polysaccharides and proteins. The uppermost layer of the outer membrane contains lipopolysaccharide. While the innermost layer of the outer membrane is a phospholipid layer which connects to lipoproteins and the peptidoglycan layer below. The outer membrane acts as a partial chemical sieve by allowing only small molecules to penetrate. The porin proteins can form channels which allow the useful molecules to go through as well as block the harmful ones such as antibiotics leading to drug resistance.

The bottom layer of gram negative cell wall is a single, thin (1-3 nm) layer of peptidoglycan. Although it acts as a rigid protective structure as previously described, its thinness gives gram negative bacteria a relatively greater flexibility and sensitivity to lysis. There is a well developed periplasmic space surrounding the peptidoglycan. This space is an important reaction site for a large and varied pool of substances that enter and leave the cell.

Bacterial growth is the division of one bacterium into two daughter cells in a process called binary fission. Providing that no mutational event occurs, the resulting daughter cells are genetically identical to the original cell. In autecological studies, bacterial growth in batch culture can be modeled with four different phases: lag phase, exponential or log phase, stationary phase and death phase (Figure 2.5).

In lag phase, bacteria adapt themselves to growth conditions. It is the period where the individual bacteria are maturing and not yet able to divide. During the lag phase of the bacterial growth cycle, synthesis of RNA, enzymes and other molecules occurs.

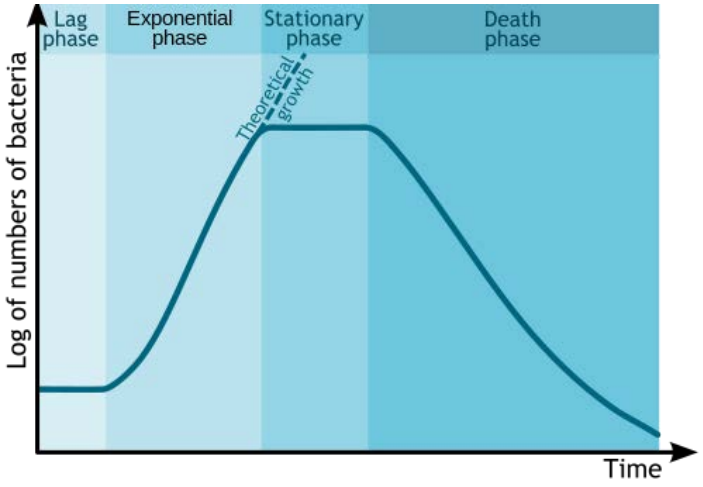

Figure 2.5 Bacterial growth curve

At exponential phase (log phase) is a period characterized by cell doubling. The number of new bacteria appearing per unit time is proportional to the present population. If growth is not limited, doubling will continue at a constant rate, both the number of cells and the rate of population increase to doubles with each consecutive time period. For this type of exponential growth, plotting the natural logarithm of cell number against time produces a straight line. The slope of this line is the specific growth rate of the organism, which is a measure of the number of divisions per cell per unit time. The actual rate of this growth (slope of the line in Figure 2.5) depends upon the growth conditions, which affect the frequency of cell division events and the probability of both daughter cells surviving. Exponential growth cannot continue indefinitely. However, because the medium is soon depleted of nutrients and enriched with wastes.

During stationary phase, the growth rate slows down as a result of nutrient depletion and accumulation of toxic products. This phase is reached as the bacteria begin to exhaust the resources that are available to them. This phase is a constant value as the rate of bacterial growth is equal to the rate of bacterial death. At death phase, bacteria run out of nutrients and die.

2.5 Antibacterial Mechanism of Chitosan

The exact mode of interaction between chitosan, its derivatives and the microorganism is still unknown, while different mechanisms have been proposed to explain antimicrobial activity. It is believed that the polycationic nature of chitosan initiates binding with the cell membrane owing to electrostatic attraction with negatively charged microbial cell membrane.

In 1991, Cuero, *et al*. [36] proposed that chitosan can bind with DNA and inhibit mRNA and protein synthesis upon penetration into the nuclei of fungi.

In 1999, Tsai, *et al*. [37] indicated that the cytoplasmic membrane of bacteria was detached from the inner part of the cell wall after chitosan treatment by using TEM analysis. Once bound to the cell surface, chitosan is thought to affect membrane permeability which leads to the leakage of proteins and other intracellular constituents of the microbial cell causing death due to the loss of essential fluids.

According to the reports from Shahidi *et al.* [38], Rabea *et al.* [39] and Raafat *et al.* [40], six main antimicrobial mechanism have been proposed: (1) Interactions between positively charged chitosan molecules and negatively charged microbial cell membranes leads to the leakage of proteinaceous and other intracellular constituents. (2) It acts as a chelating agent that selectively binds trace metals and thereby inhibits the production of toxins and microbial growth. (3) It activates several defense processes in the host tissue, acts as a water binding agent and inhibits various enzymes. (4) Binding of chitosan with DNA and inhibition of mRNA synthesis occurs via chitosan penetrating the nuclei of the micro-organisms and interfering with the synthesis of mRNA and proteins. (5) Chitosan can form an impermeable polymeric layer which disturbs the cell permeability and prevents nutrients from entering the cell. (6) Because chitosan can adsorb the electronegative substances in the cell and flocculate them, it disturbs the physiological activities of the microorganism leading to their death.

2.6 Chemical Modification of Chitosan by Click Reaction [41]

Click reaction can be referred as the joining of small units together with heteroatom linkage to generate desirable substances. The reaction must be modular, wide in scope, give very high yields, and generate only inoffensive by-products that can be easily removed and be stereospecific. The required process characteristics should be insensitive to oxygen and water, readily available starting materials and reagents, the use of no solvent or a solvent that is benign (such as water) or easily removed, and simple product isolation. The most common Click reaction used for carbon-heteroatom bond formation are: (1) cycloaddition of unsaturated species, especially 1,3-dipolar cycloaddition reactions including the Diels-Alder reaction, (2) nucleophilic substitution, particularly ring-opening reactions of strained heterocyclic electrophiles such as epoxides, (3) carbonyl chemistry of the non-aldol type, such as formation of ureas, thioureas, and (4) additions to carbon-carbon multiple bonds, especially oxidative cases such as epoxidation.

To date, Huisgen's 1,3-dipolar cycloaddition or azide-alkyne cycloaddition is one the most widely used Click reactions. A strong 1,2,3-triazole linkage can be formed by a reaction between an azide and terminal alkyne (Scheme 2.8). This

cycloaddition can take place under gently controllable condition using Cu(I) as catalyst. Besides, Cu(I)-catalyzed cycloaddition bring about selectively high yield because of effectiveness and mildness of Cu(I). These advantages of Click reaction make it widely used in synthesis and application. [42,43]

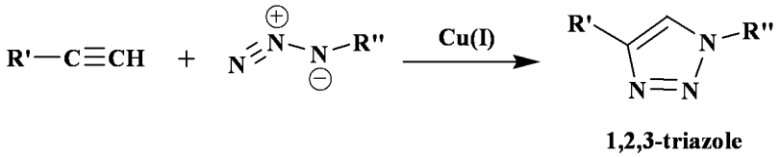

Scheme 2.8 Cu(I)-catalyzed 1,3-cycloaddition of azide and terminal alkyne

Click reaction has also been applied for chemical modification of chitosan. In 2009, Gao *et al.* [44] synthesized 6-*N,N,N*-trimethyltriazole chitosan (TCs) via Click reaction between *C*-6-azido-*N*-2-phthaloyl chitosan and propargyltrimethyl ammonium bromide, followed by removal of phthaloyl groups via hydrolysis. The TCs was used for gene delivery and showed strong DNA binding ability and high protection of DNA against nuclease degradation. In addition, the introduction of trimethyltriazole group led to significantly increase in cellular uptake as compared with the unmodified chitosan and pure gene. These results suggested that TCs could be an efficient and safe material for gene delivery.

In 2010, Zampano *et al.* [45] explored the use of Cu(I)-catalyzed [3+2] dipolar cycloaddition between *C*-6 azido-functionalized phthaloyl chitosan and 1,7-octadiyne or 1,4-diethynylbenzene as a route to regioselective crosslinking of chitosan. The preparation of *C*-6 azido-functionalized phthaloyl chitosan were carried out by two different procedures: one pot reaction (bromination and azidation) and two-step reaction (tosylation followed by azidation) (Scheme 2.9). Both methods resulted in an effective functionalization of chitosan with azido groups per pyranoside ring of 0.28 and 0.26 mol/mol for the first and second methods, respectively. The crosslinked products after removal of phthaloyl groups via after hydrolysis exhibited selective swellability in acid medium indicating that the free amino groups of chitosan were recovered after the deprotection of phthaloyl groups.

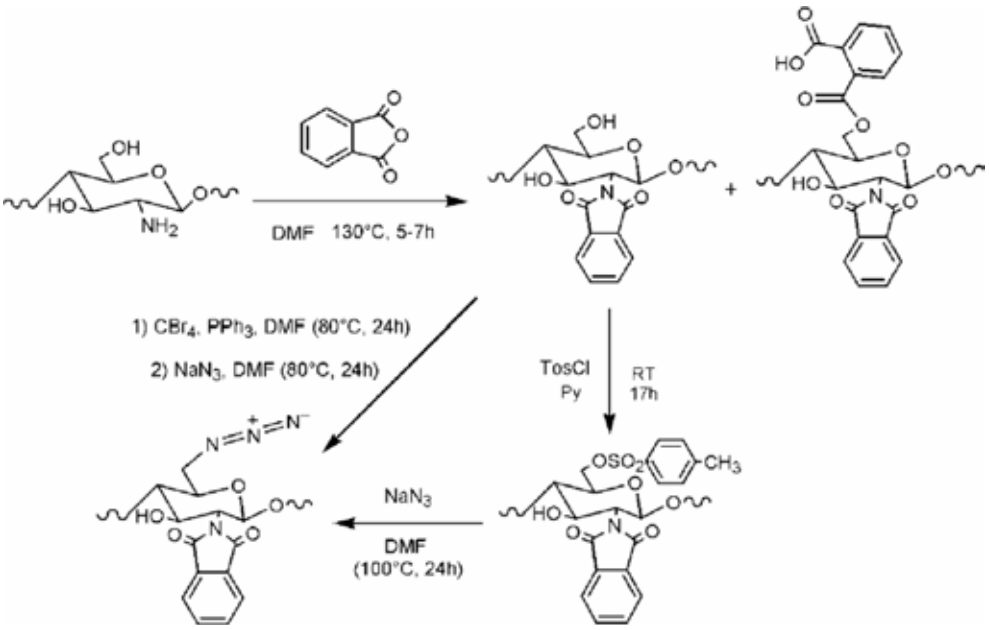

Scheme 2.9 Routes to selectively *C*-6 azido-functionalized *N*-phthaloyl-chitosan [45]

CHAPTER III
METHOD AND MATERIALS

3.1 Materials

Chitosan flakes (DD 95%, Mw 100 kDa) was purchased from Seafresh Chitosan (Lab) Co., Ltd. (Thailand). 1-Ethynylpyrene and 3-(4,5-Dimethylthiazol-2-yl)-2,5-diphenyltetrazolium bromide (MTT agent) were obtained from Alfa Aesar (USA). *N*-bromosuccinimide (NBS), copper(I)acetate, *N,N*-dimethyl-*N*-prop-2-yn, and phthalic anhydride (PhA) were obtained from Aldrich (USA). Hydrazine solution (H_2N-NH_2.H_2O) was purchased from Sigma-Aldrich (USA). 1-Bromodecane, glycidyltrimethylammonium chloride (GTMAC), *N,N*-diisopropylethylamine (DIEA), methyl iodide (MeI), sodium borohydride ($NaBH_4$), sodium iodide (NaI) and triphenylphosphine (TPP) were purchased from Fluka (Switzerland). Acetic acid, benzaldehyde, methanol (MeOH) and sodium hydroxide (NaOH) were purchased from Merck (Germany). *N,N*-dimethylformamide (DMF) and sodium azide (NaN_3) were obtained from Riedel-de Haën (Switzerland). Cyclohexane and hexane was purchased from Carlo (France). Tetrahydrofuran (THF) was obtained from ACI Labscan (Poland). All reagents and materials are analytical grade and used without further purification. *Escherichia coli (E.coli), Escherichia coli HB101 pGLO (E.coli HB101 pGLO)* and *Staphylococcus sureus (S.aureus)* were obtained from National Center for Biotechnology and Genetic Engineering and (BIOTEC), Thailand. Agar, Bacto Tryptone, Bacto Yeast Extract, Mueller-Hinton agar (MHA) and Mueller-Hinton broth (MHB) were purchased from Difco (USA).

3.2 Equipments

3.2.1 Nuclear Magnetic Resonance (NMR) Spectroscopy

^1H NMR spectra were recorded in solution of CF_3COOH/D_2O or D_2O and DMSO-d_6 using a Varian, model Mercury-400 nuclear magnetic resonance spectrometer (USA) operating at 400 MHz. Chemical shifts were reported in part per million (ppm) relative to tetramethylsilane (TMS) or using the residual protonated solvent signal as a reference.

3.2.2 Fourier Transform -Infrared Spectroscopy (FT-IR)

IR spectra were collected using a Nicolet 6700 FT-IR spectrometer with 32 scans at resolution 4 cm^{-1}. A frequency of 400-4000 cm^{-1} was collected by using TGS detector. All samples were prepared as KBr pellets.

3.2.3 Scanning Electron Microscopy (SEM)

The size and the morphology of particles were determined by scanning electron microscope (SEM, Model JEOL JSM-6480LV). The average diameter of particles was calculated by measurement of 100 random particles using Semafore software.

3.2.4 Transmission Electron Microscopy (TEM)

The morphology of particles and cross section of *E.coli* were examined by transmission electron microscope (TEM, Model JEM-2100, Japan).

3.2.5 Photon Correlation Spectroscopy (PCS)

The ζ-potential of chitosan particles was determined using a Nanosizer Nano-ZS (Malvern Instruments, UK). The particles (~10 mg) were first dispersed in 20 mL of Milli-Q water by sonication for 3 min prior to measurement. The analysis was performed at 25^{o}C using a scattering angle of 173^{o}. All data are displayed as the mean $\pm$ standard deviation and are derived from at least three independent experiments. The data were calculated using the Helmholtz-Smoluchowski equation.

3.2.6 Fluorescence Spectrophotometry

Encapsulation efficiency of particles was determined by Cary Eclipse fluorescence spectrophotometer (Agilent Technologies, USA). The excitation and emission wavelength of pyrene is 330 nm and 393 nm and the excitation and emission wavelength of nile red is 530 nm and 607 nm, respectively.

3.2.7 Fluorescence Microscopy

Fluorescent property of encapsulated quaternized chitosan particles was observed by fluorescence microscope (Cell of server Z1, Carl Zeiss, Germany).

3.2.8 Confocal Laser Scanning Microscopy (CLSM)

Interactions between the particles and bacteria as well as cellular uptake of the particles were examined by CLSM system of Nikon Digital Eclipse C1-Si (Tokyo, Japan) equipped with Plan Apochromat VC 100×, BDLaser (405 nm, Melles Griot, Carlsbad, CA, USA), a Nikon TE2000-U microscope, a 32-channel-PMT-spectral-detector and Nikon-EZ-C1 Gold Version 3.80 software was used to capture the fluorescence signals of the samples.

3.3 Methods

3.3.1 Synthesis of phthaloylchitosan (PhCS)

Chitosan (3.0 g, 17.4 mmol of $-NH_2$ group) was reacted with PhA (3 and 5 mole equivalent to amino groups of chitosan) in 20 mL DMF at 110^{o}C for 6 h under N_2 atmosphere. Then, the temperature was reduced to 60^{o}C and left overnight under N_2 atmosphere. After being precipitated in cool water and dried *in vacuo*, light yellow powder was obtained as product. The final yield was 72 %.

^{1}H NMR (DMSO-d_6) δ = 7.2-8.0 (m, 4H, aromatic of phthaloyl), 2.9 (s, 1H, -CH-N-phthaloyl) ppm.

FT-IR (KBr pellet) υ = 1,710 (C=O stretching of cyclic imide and anhydride) and 1,770 cm^{-1} (C=O stretching of cyclic imide), 720 cm^{-1} (aromatic ring).

3.3.2 Synthesis of *N,N*-dimethyl-*N*-prop-2-yn-1-yldecan-1-ammonium bromide (DPDABr) [46]

N,N-dimethyl-*N*-prop-2-yn (1.5 g, 18 mmole) was added to the solution of 1-bromodecane (3.11 mL, 15 mmole) in 10 mL THF and the reaction was continuously stirred at 50^{o}C for 2 days. After the solvent was evaporated *in vacuo* at ambient temperature, the ammonium salt was obtained as light yellow solid. The product was dissolved in THF and precipitated in cyclohexane before being dried *in vacuo*. The final yield was 84 %.

^{1}H NMR ($CDCl_3$) δ = 4.8 (s, 2H, HC≡C-$\underline{CH_2}N^+$), 3.4 (s, 6H, -N^+-$\underline{(CH_3)_2}$), 2.9 (s, 1H, $\underline{CH}$≡C-), 1.2-1.4 (m, 9H, -N^+-$\underline{(CH_2)_9}$-CH_3), 0.8 (t, 3H, *J*= 6.80 Hz, -CH_2-$\underline{CH_3}$) ppm.

3.3.3 Preparation of amphiphilic chitosan particles

3.3.3.1 Particles having phthaloyl group as hydrophobic entity and *N*-[(2-hydroxyl-3-trimethylammonium)]propyl (HTAP) group as hydrophilic entity

PhCS (0.4 g), obtained from section 2.3.1, was dissolved in 8 mL DMF at ambient temperature. Then, pH of the solution was adjusted by adding 0.1 M NaOH (aq) to 9. GTMAC (3 mole equivalent to amino groups of chitosan) was added and the reaction was stirred at 70°C for 24 h. After dialysis the solution against deionized water for 4 days and lyophilization, the particles were formed. The particles having HTAP as the hydrophilic entity and phthaloyl group as the hydrophobic entity are defined as Ph-CS-HTAP. The final yield was 96 %.

^{1}H NMR (CF_3COOH/D_2O) δ = 7.2-8.0 (m, 4H, aromatic), 3.00-3.05 (s, 9H, $N^+(\underline{CH_3})_3$), 2.9 (s, 1H, -<u>CH</u>-N-phthaloyl) ppm.

FT-IR (KBr pellet) υ = 1,720 cm^{-1} (C=O stretching of cyclic imide and anhydride), 725 cm^{-1} (aromatic ring), 1,475 cm^{-1} (C-H deformation of $N^+(CH_3)_3$).

3.3.3.2 Particles having pyrene as hydrophobic entity and HTAP group as hydrophilic entity

NBS (10 mole equivalent to amino groups of chitosan) and TPP (10 mole equivalent to amino groups of chitosan) were added to a solution of PhCS (0.5 g, 2.9 mmol of $–NH_2$ group) in 50 mL DMF. The mixture was stirred at 80°C for 2 h under N_2 atmosphere. Dark brown powder was obtained as product after precipitation in ethanol and dried *in vacuo*. Then 0.4 g of product was reacted with NaN_3 (1.51 g, 10 mole equivalent to amino groups of chitosan) in 40 mL DMF at 80°C for 4 h under N_2 atmosphere before being precipitated in ethanol and dried *in vacuo*. The *C-6*-azido-*N*-phthaloylchitosan (N_3-PhCS) was obtained as brown powder. Click reaction between the N_3-PhCS (0.1 g) and 1-ethynylpyrene (39.3 mg, 0.25 mole equivalent to amino groups of chitosan) was conducted by using Cu(I) (3.19 mg, 0.15 mole equivalent to 1-ethynylpyrene) as catalyst and DIEA (0.5 mole equivalent to amino groups of chitosan) as base for 24 h under N_2 atmosphere to yield pyrene-functionalized PhCS (Pyr-PhCS) obtained as yellow powder after dialysis against

deionized water for 4 days and lyophilization. Removal of phthaloyl groups by hydrolysis using hydrazine solution (64-65% H_2N-$NH_2.H_2O$) was performed by stirring 1 g of Pyr-PhCS in 100 mL of hydrazine solution at 80^oC for 4 h under N_2 atmosphere. After dialysis against deionized water for 4 days and lyophilization, yellow powder was obtained as product. Finally, the product (15.0 mg) was reacted with GTMAC (23.5 µL, 2 mole equivalent to amino groups of chitosan) at 70^oC for 24 h. Particles which are designated Pyr-CS-HTAP were obtained after dialysis against deionized water for 4 days and lyophilization. The final yield was 98 %.

^{1}H NMR (DMSO-d_6) δ = 8.0-8.8 (m, 9H, aromatic of pyrene), 3.00-3.05 (s, 9H, $N^+(\underline{CH_3})_3$) ppm.

FT-IR (KBr pellet) υ = 2,100 cm^{-1} ($^-N=N^+=N^-$ stretching), 1,480 cm^{-1} (C-H deformation of quaternary ammonium), 1,710 cm^{-1} (C=O stretching of cyclic imide and anhydride).

3.3.3.3 Particles having phthaloyl group as hydrophobic entity and 4-[(*N*-decyl-*N*,*N*-dimethylammonium methyl)]triazolyl (DDAMT) as hydrophilic Entity

Click reaction between the N_3-PhCS obtained from 2.3.3.2 (0.1 g) and DPDABr obtained from 2.3.2 (0.5 mole equivalent to amino groups of chitosan) took place by using Cu(I) (15 mole% of alkyne) as catalyst and DIEA (0.5 mole equivalent to amino groups of chitosan) as base for 24 h under N_2 atmosphere to yield DDAMT-functionalized PhCS (Ph-CS-DDAMT) obtained as light brown powder after dialysis against deionized water for 4 days and lyophilization. The final yield was 90 %.

^{1}H NMR (CF_3COOH/D_2O) δ = 3.00-3.05 (s, 9H, $N^+(\underline{CH_3})_3$), 0.8-1.0 (m, 9H, $-N^+-(\underline{CH_2})_9-CH_3$), 0.6 (t, 3H, *J*= 6.80 Hz, $-CH_2-\underline{CH_3}$) ppm.

FT-IR (KBr pellet) υ = 2,100 cm^{-1} ($^-N=N^+=N^-$ stretching), 2,130 cm^{-1} (-C≡C- stretching), 1,720 cm^{-1} (C=O stretching of cyclic imide and anhydride), 2,930 cm^{-1} (C-H stretching of decyl groups), 1,480 cm^{-1} (C-H deformation of quaternary ammonium).

3.3.4 Encapsulation of fluorescent dye by amphiphilic chitosan particles

Nile red (0.1 mole equivalent to amino groups of chitosan) or pyrene (0.25 mole equivalent to amino groups of chitosan) was dissolved in 1 mL DMF. The dye solution was then added dropwise to the dispersed particles in 10 mL deionized water. After sonication for 30 minutes, the solution/dispersion was dialyzed against deionized water for 1 day and lyophilized. In the case of nile red-encapsulated particles, the particles were washed thoroughly with acetone until the red solution turned to colorless to eliminate the non-encapsulated dye adsorbed on the particle surface. In the case of pyrene-encapsulated particles, the supernatant was colorless and pyrene is not water-soluble. The absence of white precipitate upon an addition of the supernatant to deionized water can be used as an evidence for complete removal of non-encapcapsulated pyrene.

To determine encapsulation efficiency of particles, combined solution of the supernatant inside the dialysis bag and that obtained after washing were subjected to fluorescence intensity measurements by fluorescence spectrophotometry. The excitation and emission wavelength of pyrene were 330 and 393 nm, respectively. And the excitation and emission wavelength of nile red were 530 and 607 nm, respectively. Concentration of each dye was calculated based on the pre-determined calibration curve shown in Appendix A. (Figure A-1 and A-2). The data are shown in Table A-1.

3.3.5 Determination of antibacterial activity

All glasswares used for the tests were sterilized in an autoclave at 121°C for 15 min before use. Mueller-Hinton broth dissolved in deionized water was also autoclaved for 15 min at 121°C. The broth was stored at 4 °C before use. Mueller-Hinton agar dissolved in deionized water (5 mL) was transferred in to each test tube before autoclaved for 15 min at 121°C. The tubes are placed in a slanted position to allow the agar to solidify. The agar slant was stored at 4^{o}C before use. All particles were sterilized by exposing to UV radiation for 60 min prior to the tests.

S. aureus and *E. coli* were used as gram positive and gram negative bacteria, respectively. A loopful of bacteria were streaked on agar slant, then incubated at 37°C in an incubator (growth carbinet, Sanyo, Japan) for 24 h. Sterile deionized water (10

mL) was added in the tube containing agar slant to obtain bacterial suspension. The optical density of the suspended bacteria in sterile deionized water was determined by UV-visible spectrophotometer (UVmini-1240 SHIMADZU, Japan) at a wavelength of 600 nm (OD_{600}). The value was adjusted by sterile deionized water to 0.5 and 0.1 for viable cell counting and clear zone method, respectively.

3.3.5.1 Viable cell counting method

Particles (2.5 mg) were added to test tubes each containing 5 mL of broth. Then 50 µL of the freshly prepared bacterial suspension (OD_{600} = 0.5) was inoculated to each tubes. All protocols were done under aseptic conditions. After that, the tubes were incubated at 37^{o}C for 24 h and at a shaking speed of 110 rpm (temperature controlled water bath shaker, Memmert (Germany)). Then, the mixture (100 µL) was diluted to 10^6 times. A 100 µL of diluted mixture was spreaded onto ager plates before incubating at 37^{o}C for 18 h. The colonies of viable bacteria were counted. The results were shown as mean colony forming units per volume (CFU/mL) after multiplication with the dilution factor.

3.3.5.3 Statistical Analysis

All data obtained from the tests of antibacterial activity are expressed as mean ± standard deviation (SD) of a representative of three independent experiments carried out in triplicate. Statistical analysis was performed using the Statistical Package for the Social Science (SPSS) version 17.0 software. Statistical comparisons made by One-Way Analysis of Variance (ANOVA) with the Least Square Difference (LSD) tests were used for post hoc evaluations of differences between groups. Statistical significance was associated with the value of $p < 0.01$.

3.3.6 Cytotoxicity test

Mouse leukaemic monocyte macrophage cell line (Raw 264.7) (purchased from American Type Culture Collection (ATCC)) were seeded in 96-well flat-bottomed plates at a density of 10^4 cells and incubated at 37˚C in humidified atmosphere (5% CO_2) with Dulbecco's Modified Eagle Medium (DMEM) supplemented with 10% (v/v) of fetal bovine serum (FBS) and 0.01% (v/v) of

penicillin and 0.05% (v/v) of streptomycin. The particles at various concentrations in a range of 0-100 µg/mL were then added to 96-well plate and incubated at 37˚C for 24 h. The MTT agent was added in each well and after incubation for 4 h, the 96-well plate was centrifuged. Then, the supernatant of each well was transferred to a new 96-well plate and the UV absorbance of each well at 540 nm was measured with a microplate reader (Biochrom, United Kingdom). Each concentration of particles was tested in three replicates per plate. The results were expressed as a percentage of the viable cells.

3.3.7 Cellular Uptake of Particles

Mouse leukaemic monocyte macrophage cell line (Raw 264.7) (purchased from American Type Culture Collection (ATCC)) were seeded in 25 cm^2 vented culture flasks and incubated at 37˚C in humidified atmosphere (5% CO_2) with Dulbecco's Modified Eagle Medium (DMEM) supplemented with 10% (v/v) of fetal bovine serum (FBS) and 0.01% (v/v) of penicillin and 0.05% (v/v) of streptomycin.

Raw 264.7 cells, at a density of 3 x 10^5 cells per well, were seeded in 6-well plates on cover slips and incubated overnight at 37°C in humidified atmosphere (5% CO_2). The samples (2000 ppm) was added directly to cells in each well (PBS was used as a negative control). The sample was allowed to interact with cells for 4 h and 24 h at 37°C in a humidified atmosphere (5% CO_2). Cells were washed and replaced with fresh PBS pH 7.4 three times, and fixed with 1 ml of 4% paraformaldehyde for 15 min and washed with fresh PBS pH 7.4. Cells were incubated with 1 mL of 10 µg/mL Dapi solution for 10 min. This step was followed by washing with fresh PBS pH 7.4 before being subjected to CLSM analysis.

CHAPTER IV
RESULTS AND DISCUSSION

This chapter is divided into 2 parts. The first part (section 4.1-4.4) concentrates on the synthesis, preparation and characterization of amphiphilic chitosan particles. The second part (section 4.5-4.6) reveals the results of tests on antibacterial activity, cytotoxicity and cellular uptake of selected amphiphilic chitosan particles.

4.1 Synthesis of Phthaloylchitosan (PhCS)

Phthaloyl groups have been widely used as hydrophobic entity in the synthesis of amphiphilic chitosan because of its good reactivity is known to effectively induce particle formation by self-assembly. [27,28,29,31] Phthaloyl groups are attached to chitosan backbone via ring opening of PhA by amino groups and hydroxyl groups of chitosan (Scheme 4.1). Under neutral to alkaline conditions, amino groups are more nucleophilic than hydroxyl groups because the electronegativity of nitrogen is less than oxygen. However, the nucleophilicity of the amino groups became inferior in acidic media in which amino groups can be protonated. If amino groups act as nucleophiles, phthalimide is obtained as product (Scheme 4.2). The phthalimide is stable cyclic imide that has planar rearrangement of the aromatic ring leading to π−π stacking interactions between phthalimido groups, the important factor for self-assembly. But if hydroxyl groups acts as nucleophiles, the product is an anhydride (Scheme 4.3). The cyclic ester is unstable and can be hydrolyzed to carboxyl group.

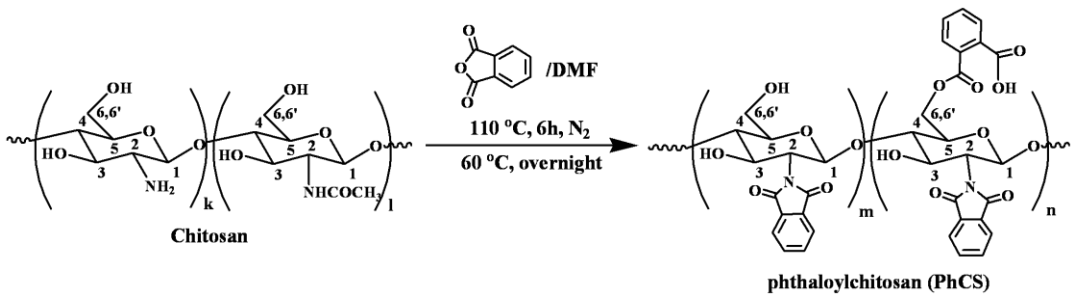

Scheme 4.1 Synthesis of PhCS.

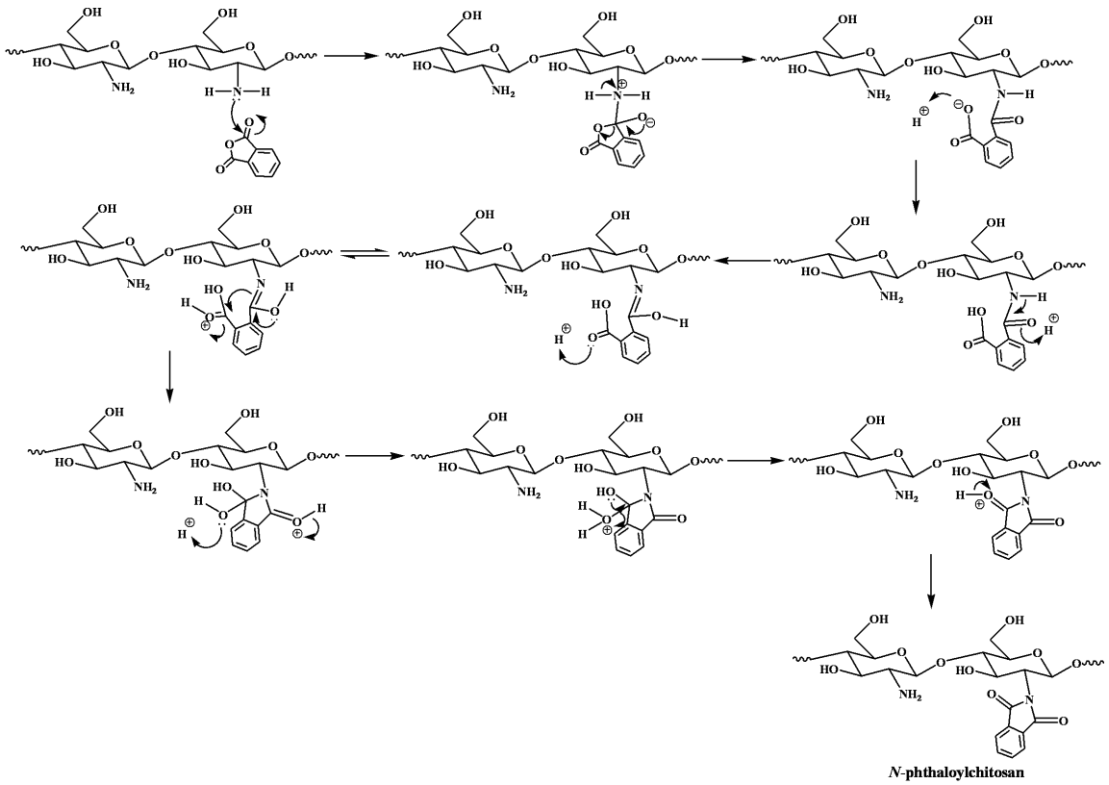

Scheme 4.2 Mechanism of PhA ring opening by amino groups of chitosan that yields *N*-phthaloylchitosan

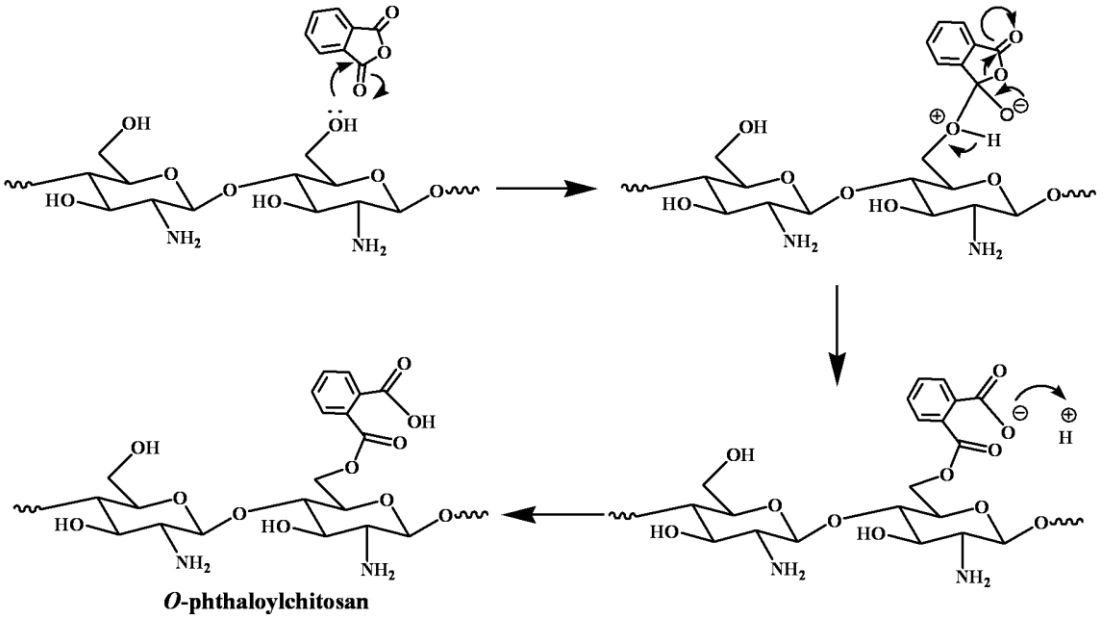

Scheme 4.3 Mechanism of PhA ring opening by hydroxyl groups of chitosan that yields *O*-phthaloylchitosan

Figure 4.1 shows ^{1}H NMR spectra of PhCS and chitosan. The signal in a region of 7.2-8.0 ppm **(**Figure 4.1b**)** can be assigned to aromatic protons of phthaloyl groups. Degree of phthaloyl group substitution (%DS_{Ph}) on chitosan can be calculated from the relative ratio between the peak integration of aromatic protons at 7.2-8.0 ppm and the peak integration of proton at C-2 of chitosan at 2.9 ppm using equation 4.1. The calculated %DS_{Ph} of 128.8±1.8 % was obtained implying that phthaloyl substitution took place not only at C-2 (*N*-phthaloyl) but also at C-6 (*O*-phthaloyl) positions of chitosan.

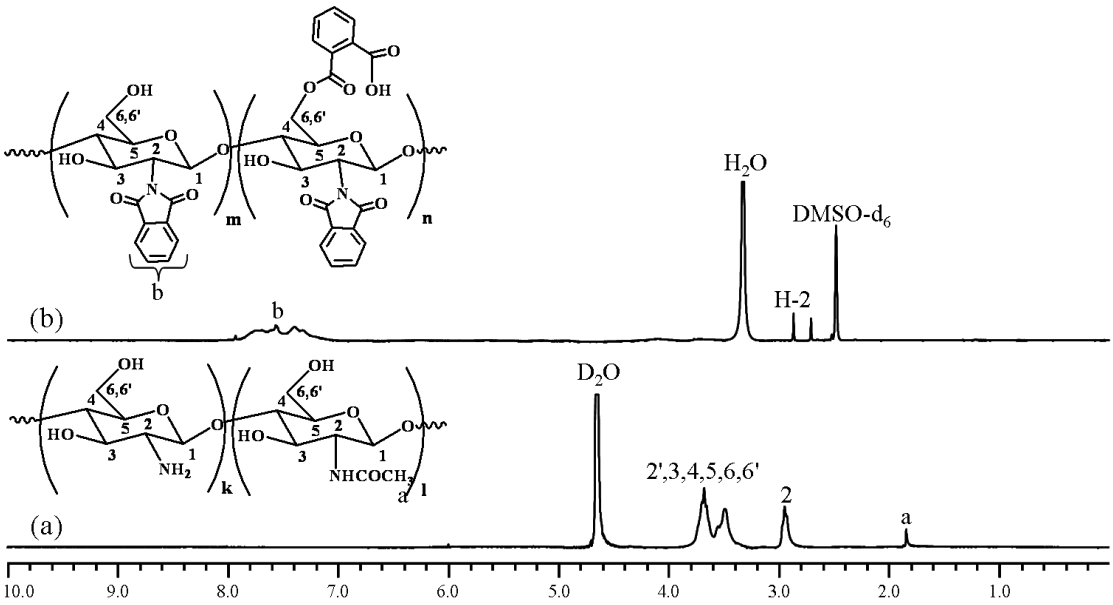

Figure 4.1 ^{1}H NMR spectra of (a) chitosan and (b) PhCS.

$$\%DS_{Ph} = \left\{ \frac{\text{integral of } C_6H_4 \text{ /4}}{\text{integral of H-2 /1}} \right\} \text{ x 100} \qquad (4.1)$$

The functionalities of modified chitosan derivatives can be verified by FT-IR analysis. In comparison with chitosan (Figure 4.2a), a new peak appearing at 720 cm^{-1} in the spectrum of PhCS (Figure 4.2b) can be assigned to out of plane C–H deformation of aromatic rings of phthaloyl groups. In addition, a decrement of N-H bending of primary amine in chitosan at 1,600 cm^{-1} and an emergence of peaks at

1,710 cm^{-1} and 1,770 cm^{-1} attributed to C=O stretching of cyclic imide also confirmed the success of phthaloyl attachment on chitosan backbone.

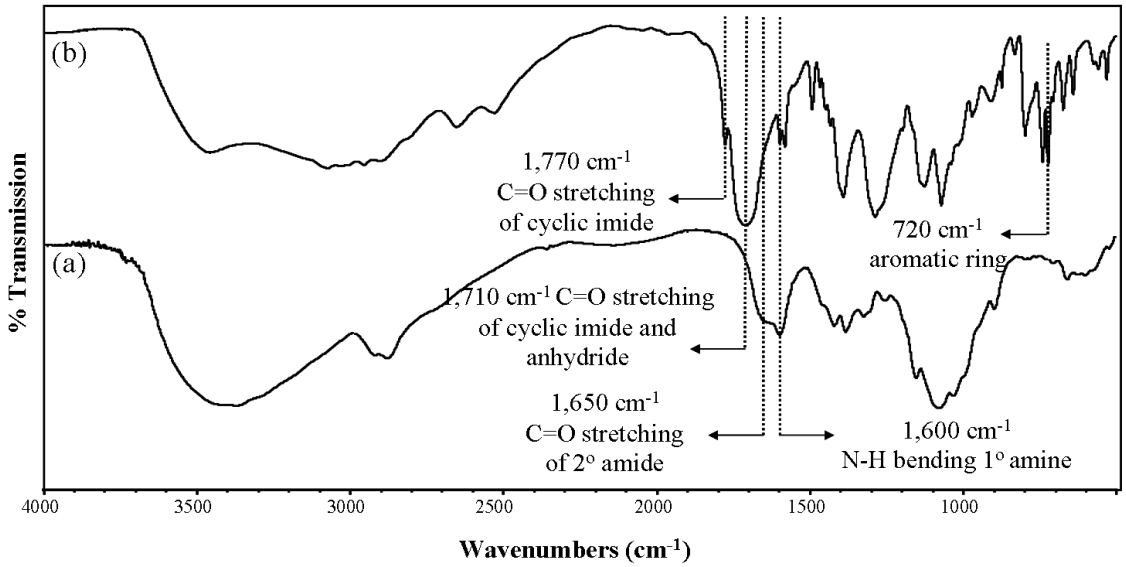

Figure 4.2 FT-IR spectra of (a) chitosan and (b) PhCS.

4.2 Synthesis of *N,N*-dimethyl-*N*-prop-2-yn-1-yldecan-1-ammonium bromide (DPDABr)

Alkylation of *N,N*-dimethyl-*N*-prop-2-yne with bromodecane leads to the formation of quaternary ammonium salt derivative, *N,N*-dimethyl-*N*-prop-2-yn-1-yl decan-1-ammonium bromide (DPDABr) (Scheme 4.4). As shown in Figure 4.3, the signal at chemical shift of 1.2-1.4 and 0.8 ppm attributed to protons of methylene and methyl groups, respectively from introduced decyl group. Clear signal at chemical shift of 2.9 ppm can be assigned to proton from terminal alkyne. And the signal at chemical shift of 3.4 ppm indicated the protons of two methyl groups from quaternary ammonium entity. This reagent will later be used for the preparation of amphiphilic chitosan having 4-[(*N*-decyl-*N,N*-dimethylammonium methyl)]triazolyl (DDAMT) as hydrophilic entity.

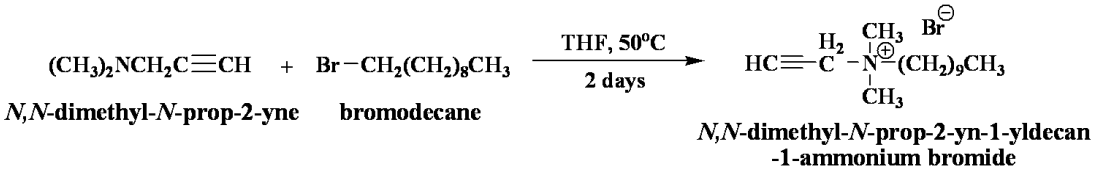

Scheme 4.4 Synthesis of DPDABr

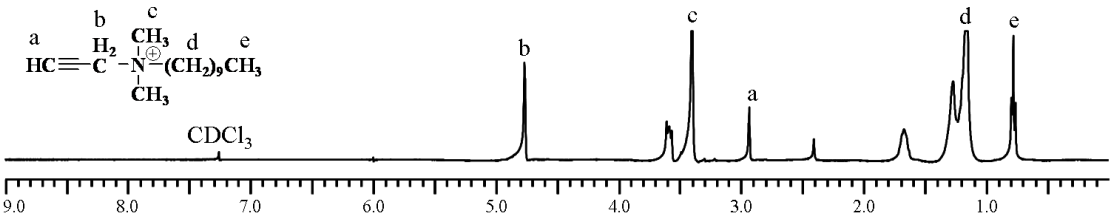

Figure 4.3 ^{1}H NMR spectrum of DPDABr.

4.3 Preparation of Amphiphilic Chitosan Particles

4.3.1 Particles having Phthaloyl Group as Hydrophobic Entity and HTAP Group as Hydrophilic Entity (Ph-CS-HTAP)

The positively charged HTAP group can be attached to the PhCS via ring opening of glycidyltrimethylammonium chloride (GTMAC) by amino and hydroxyl groups of chitosan and yield Ph-CS-HTAP. It is known that GTMAC reacts with amino groups of chitosan under acidic condition but preferably reacts with hydroxyl groups under neutral and alkaline conditions. [47] Due to the fact that most of amino positions of PhCS should be occupied by phthaloyl groups and the reaction was selectively performed under basic condition, HTAP groups should be mostly substituted at hydeoxyl positions (Scheme 4.5). The particle formation can be induced by self-assembly of the resulting product in water.

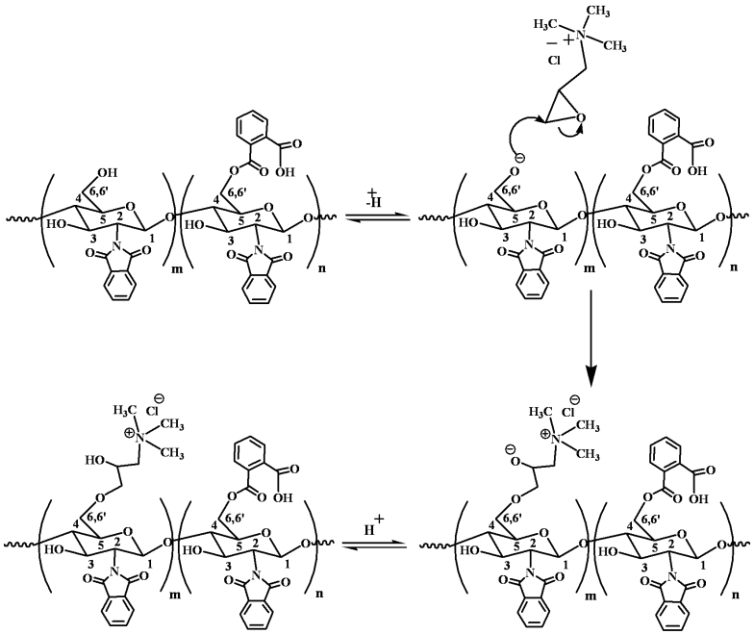

Scheme 4.5 Mechanism of GTMAC ring opening by hydroxyl groups of PhCS that yields Ph-CS-HTAP

From Figure 4.4, the signals at chemical shift of 7.2-8.0 ppm in the spectrum of Ph-CS-HTAP can be assigned to the protons of aromatic ring from phthaloyl groups. The appearance of quaternary ammonium groups in Ph-CS-HTAP are indicated by the signals at chemical shift of 3.00-3.05 ppm. Degree of HTAP substitution ($\%DS_{HTAP}$) of 73.3 ± 3.1% was calculated from the relative ratio between the integration of protons from quaternary ammonium group ($-N^{+}(CH_3)_3$) and the peak integration of proton at C-2 of chitosan at 2.9 ppm using equation 4.2.

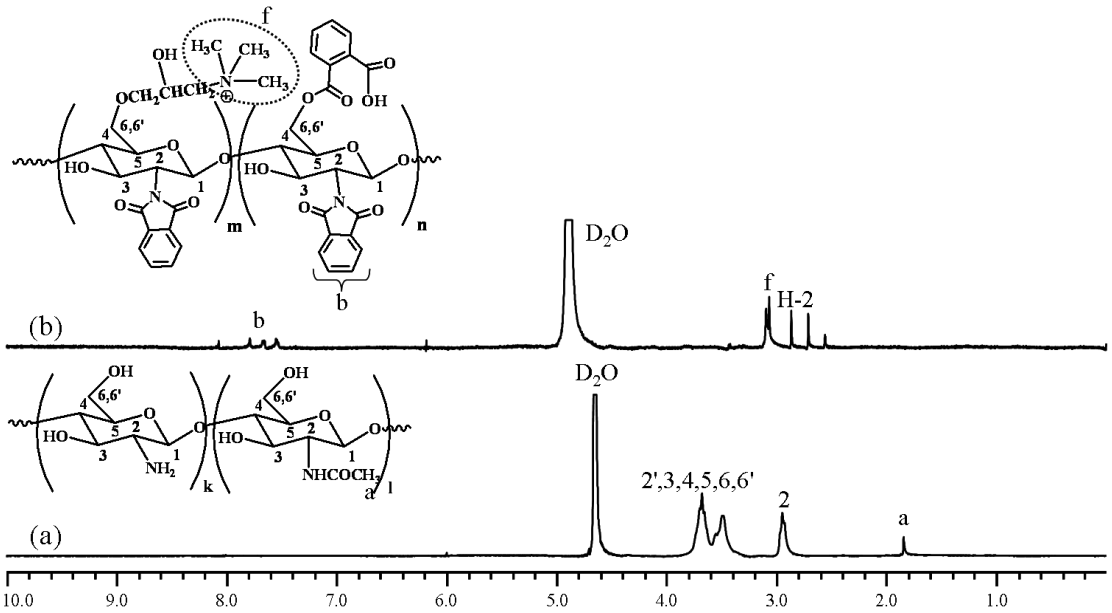

Figure 4.4 ^{1}H NMR spectra of (a) chitosan and (b) Ph-CS-HTAP.

$$\%DS_{HTAP} = \left\{ \frac{\text{integral of } N^{+}(CH_3)_3 /9}{\text{integral of H-2 /1}} \right\} \text{ x } 100 \qquad (4.2)$$

The Ph-CS-HTAP particles were also characterized by FT-IR as shown in Figure 4.5a, the signal of C-H deformation at 1,475 cm^{-1} can be assigned to quaternary ammonium functionality. The signal at 725 cm^{-1} of out of plane C-H deformation of the aromatic ring and peaks at 1,710 cm^{-1} and 1,770 cm^{-1} attributed to C=O stretching of cyclic imide indicated the existence of phthaloyl groups.

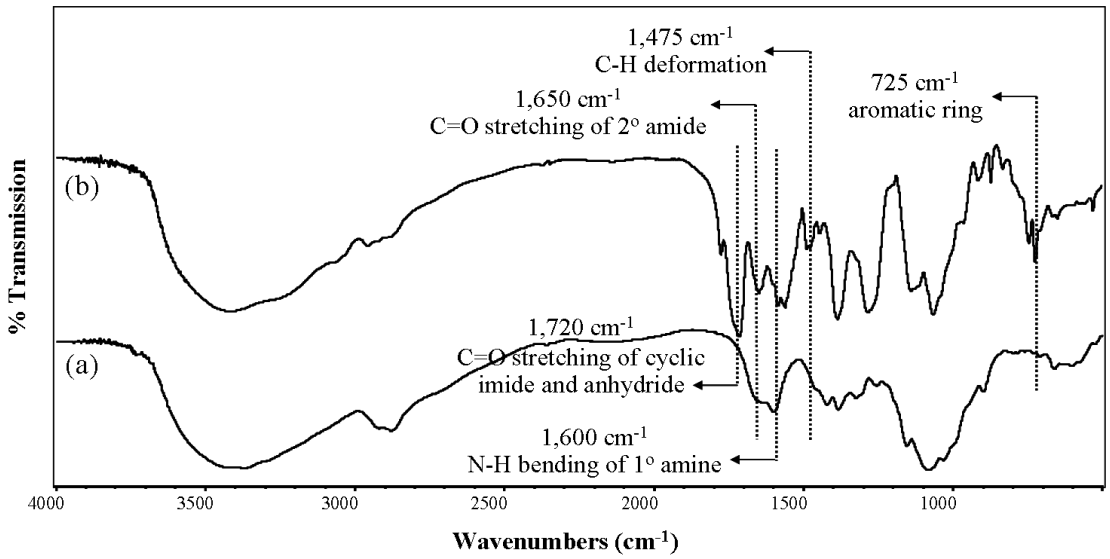

Figure 4.5 FT-IR spectra of (a) chitosan and (b) Ph-CS-HTAP.

4.3.2 Particles having Pyrene as Hydrophobic Entity and HTAP Group as Hydrophilic Entity (Pyr-CS-HTAP)

As shown in Scheme 4.6, PhCS was first subjected to bromination before reacting with NaN_3 to form N_3-PhCS. Click reaction by 1,3-dipolar cycloaddition between the N_3-PhCS and 1-ethynylpyrene was performed using Cu(I) as catalyst and DIEA as base (Scheme 4.7) to yield pyrene-functionalized PhCS (Pyr-PhCS). Phthaloyl groups from Pyr-PhCS was then removed by hydrolysis with hydrazine solution to recover back the free amino groups which are readily available for further reaction with GTMAC to form Pyr-CS-HTAP particles having pyrene as hydrophobic entity and HTAP as hydrophilic entity upon final dialysis.

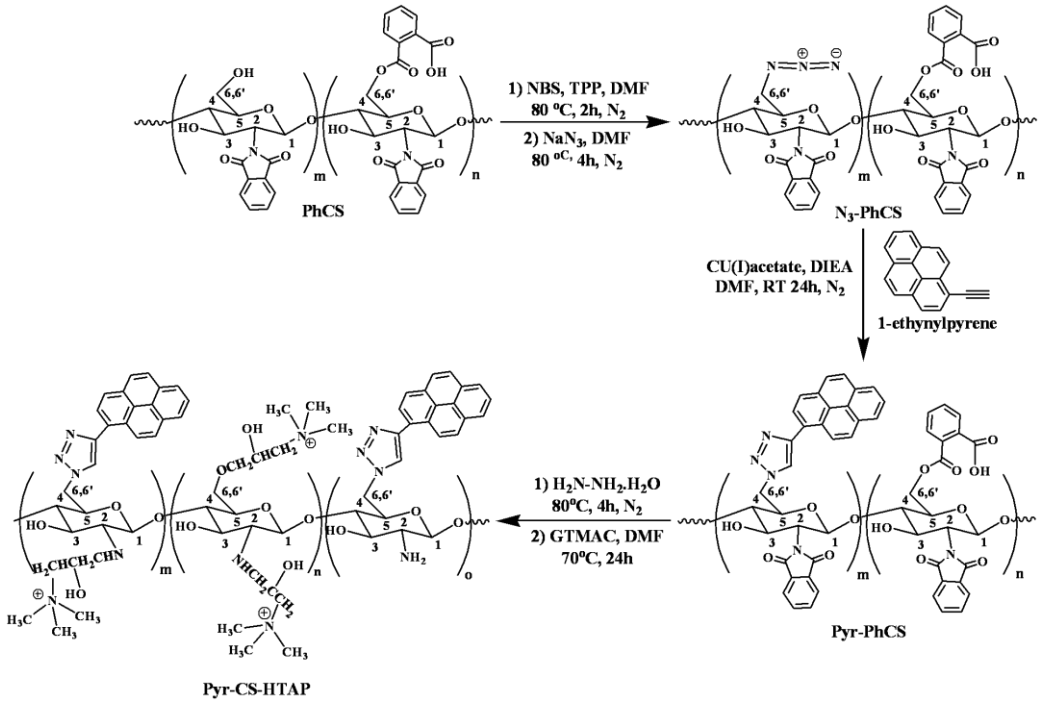

Scheme 4.6 Preparation of Pyr-CS-HTAP.

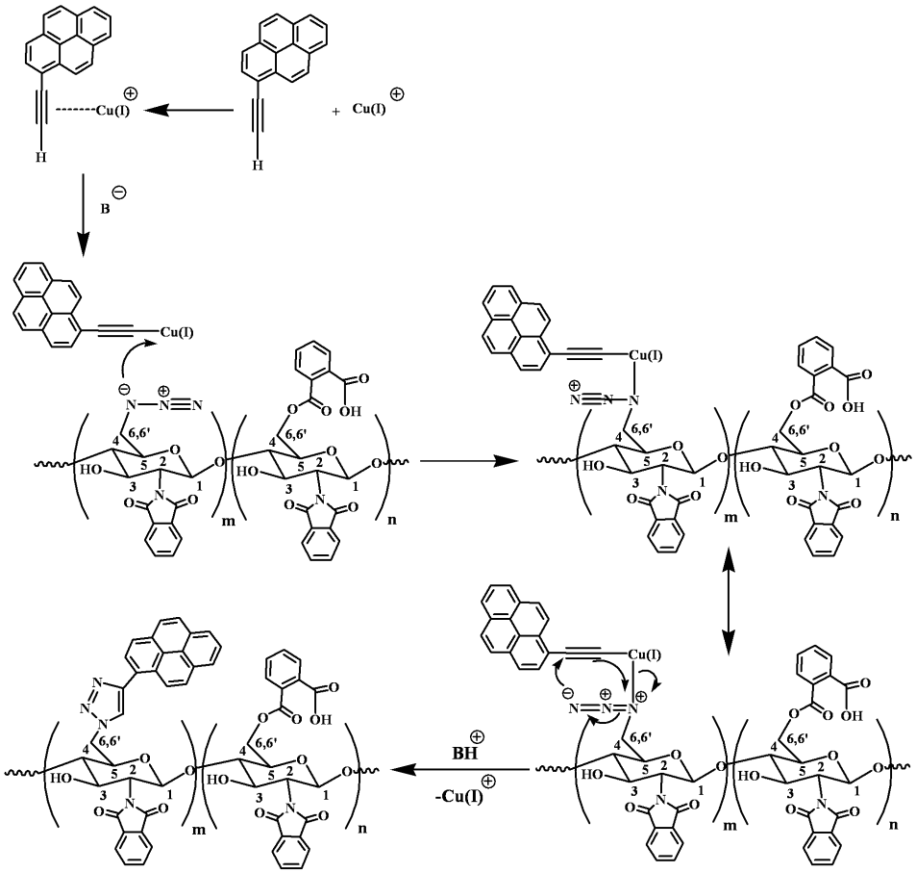

Scheme 4.7 Mechanism of click reaction between 1-ethynylpyrene and N_3-PhCS

^{1}H NMR spectrum of Pyr-CS-HTAP is shown in Figure 4.6c in comparison with those of chitosan and PhCS (Figure 4.6a-b). The signal at chemical shift 8.0-8.8 ppm can be assigned to protons of pyrene ring attached to chitosan via click reaction while the signal at chemical shift 3.00-3.05 ppm can be attributed to methyl protons of HTAP groups introduced by the reaction with GTMAC. It is obvious that the chemical shift 7.2-8.0 ppm assigned to protons of aromatic ring from phthaloyl groups found in PhCS (Figure 4.6b) cannot be found in the spectrum of Pyr-CS-HTAP (Figure 4.6c) indicating that the removal of phthaloyl groups by hydrolysis was complete. Degree of pyrene substitution (%DS_{Pyr}) calculated from the relative ratio between the peak integration of protons of pyrene ring (The signal at chemical shift 8.0-8.8 ppm) and the peak integration of proton at C-2 of chitosan at 2.9 ppm using equation 4.3 was found to be 61.1± 0.6%. Using equation 4.2, %DS_{HTAP} of Pyr-CS-HTAP was found to be 48.8 ± 0.2%.

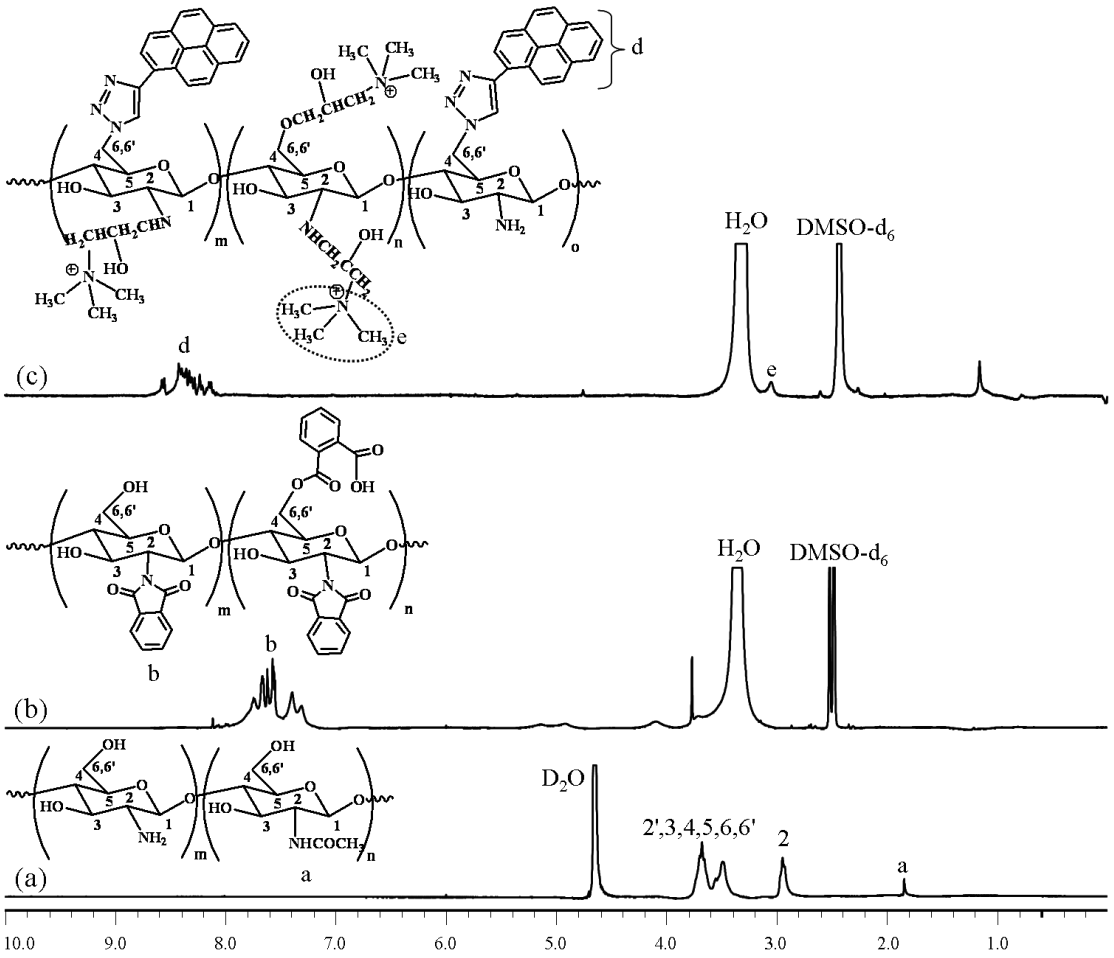

Figure 4.6 ^{1}H NMR spectra of (a) chitosan, (b) PhCS, and (c) Pyr-CS-HTAP

$$\%DS_{Pyr} = \left\{ \frac{\text{integral of } C_{16}H_9 \,/9}{\text{integral of H-2}\,/1} \right\} \text{x } 100 \qquad (4.3)$$

FT-IR technique was used to monitor the stepwise functionalization. As shown in Figure 4.7, a characteristic stretching of azide group in N_3-PhCS emerges at 2100 cm^{-1} (Figure 4.7c) and disappears after the click reaction with ethynylpyrene (Figure 4.7d). The presence of C-H deformation peak of $-N^+(CH_3)_3$ at 1480 cm^{-1} and the absence of C=O stretching at 1710 cm^{-1} (found in PhCS, Figure 4.7b) in the spectrum of Pyr-CS-HTAP (Figure 4.7d) verified the success of HTAP incorporation and the complete removal of phthaloyl entities, respectively.

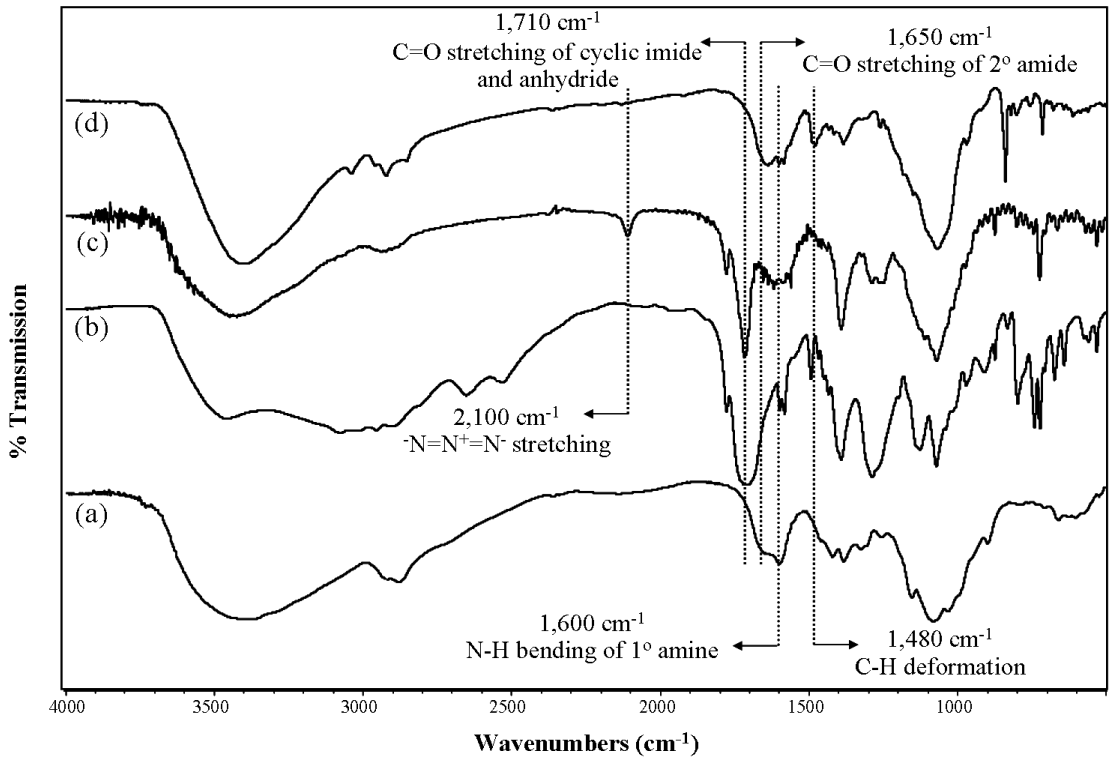

Figure 4.7 FT-IR spectra of (a) chitosan, (b) PhCS, (c) N_3-PhCS, and (d) Pyr-CS-HTAP.

4.3.3 Particles having Phthaloyl Group as Hydrophobic Entity and 4-[(*N*-decyl-*N*,*N*-dimethylammonium methyl)]triazolyl (DDAMT) as Hydrophilic Entity (Ph-CS-DDAMT)

Amphiphilic chitosan particles having 4-[(*N*-decyl-*N,N*-dimethylammonium methyl)]triazolyl (DDAMT) as hydrophilic entity can be prepared by clicking N_3-PhCS with DPDABr (Scheme 4.8). The obtained particles, Ph-CS-DDAMT, obtained after dialysis were characterized by ^{1}H NMR and FT-IR.

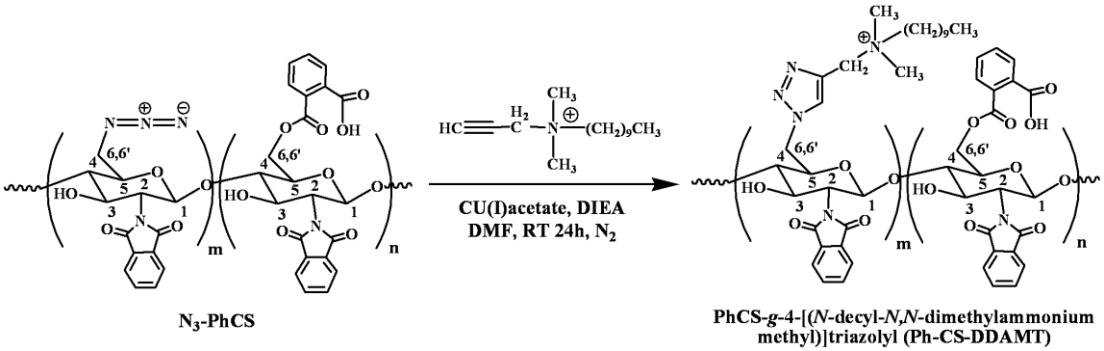

Scheme 4.8 Preparation of Ph-CS-DDAMT.

As shown in Figure 4.8, the signal at chemical shift 0.6 and 0.8-1.0 ppm can be assigned to methyl and methylene protons of decyl group, respectively. The signal at 3.00-3.05 ppm indicated protons of methyl groups from quaternary ammonium group (Figure 4.8c). Degree of DDAMT substitution (%DS_{DDAMT}) of Ph-CS-DDAMT can be calculated from relative ratio between the peak integration of methyl protons from decyl group and the peak integration of proton at C-2 of chitosan at 2.9 ppm using equation 4.4. By using the mole ratio of DPDABr to amino groups of chitosan of 0.5, %DS_{DDAMT} of 16.8 ± 0.2% was obtained. It is anticipated that higher %DS_{DDAMT} can be achieved if greater mole ratio was applied.

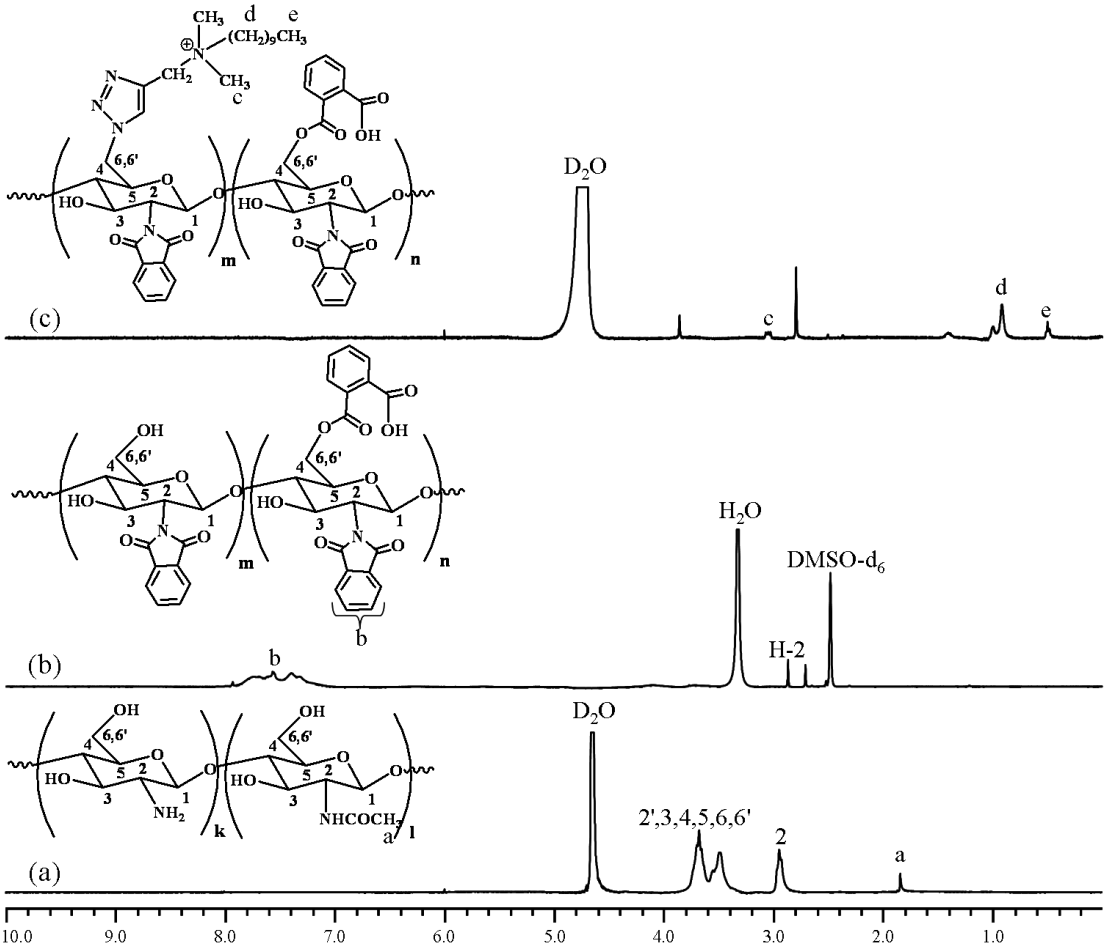

Figure 4.8 ^{1}H NMR spectra of (a) chitosan, (b) PhCS, and (c) Ph-CS-DDAMT.

$$\%DS_{DDAMT} = \left\{ \frac{\text{integral of } N^{+}(CH_2)_9\underline{CH_3}\ /3}{\text{integral of H-2 /1}} \right\} \text{ x } 100 \qquad (4.4)$$

The functionalities of Ph-CS-DDAMT were verified by FT-IR analysis as shown in Figure 4.9. The disappearance of the characteristic azide stretching (found in N_3-PhCS, Figure 4.9c) in Figure 4.9d confirmed the completeness of click reaction. Besides, the C-H deformation peak of $-N^{+}(CH_3)_2$ at 1,480 cm^{-1} also verified the successful introduction of quaternary ammonium groups via click reaction. The strong C-H stretching peak at 2,930 cm^{-1} can be assigned to the decyl group tagged on quaternary ammonium entity of DDAMT. In addition, the hydrophobic entity,

phthaloyl group, still remained intact as can be realized from the presence of C=O stretching peak at 1,720 cm^{-1}.

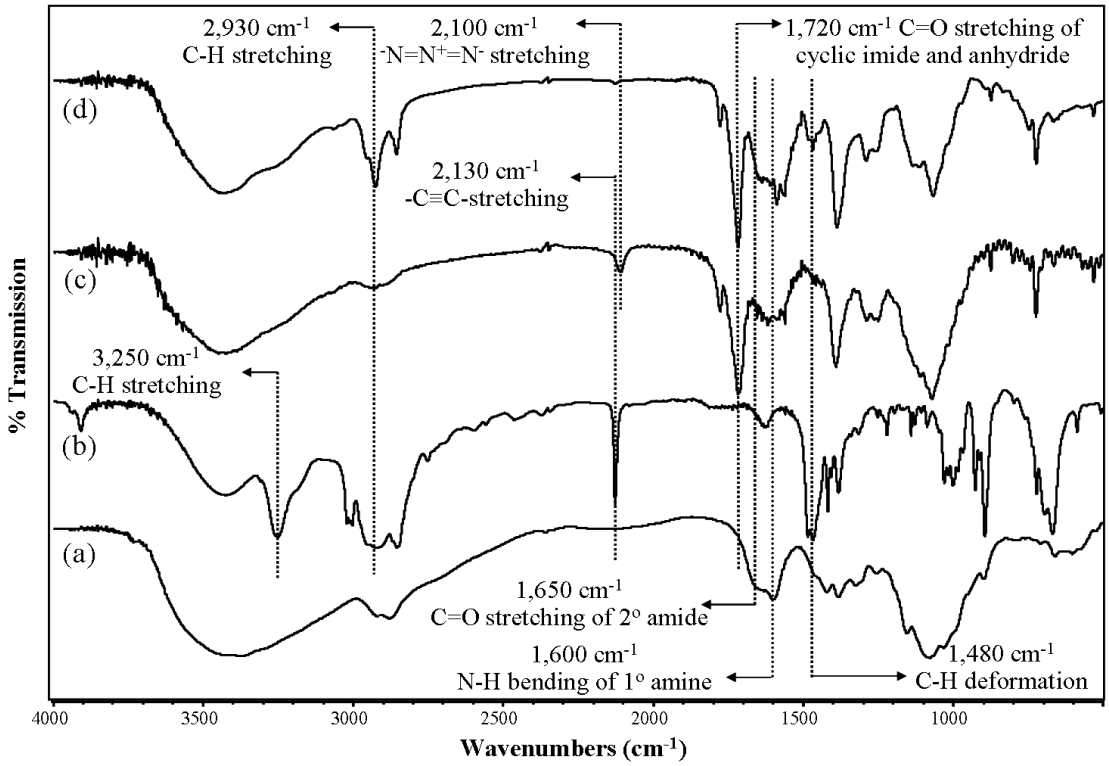

Figure 4.9 FT-IR spectra of (a) chitosan, (b) DPDABr, (c) N_3-PhCS, and (d) Ph-CS-DDAMT.

4.4 Characterization of Amphiphilic Chitosan Particles

4.4.1 Physical Characteristics

As determined by SEM (Figure 4.10), all amphiphilic chitosan particles are quite spherical in shape. Ph-CS-HTAP have relatively smooth surface with a broad size variation of 1.50±0.69 μm. Their morphology resembles that of the amphiphilic chitosan particles having phthaloyl group as hydrophobic entity and mPEG as hydrophilic entity (Ph-CS-mPEG) as previously reported by others [27,28,29] but with much greater size. This may be due to the fact that mPEG is polymeric entity that can provide steric stabilization to the amphiphilic chitosan, thus promotes the self assembly process, perhaps much more efficiently than the HTAP group and yields much smaller particles. Nevertheless, the Ph-CS-HTAP is positive in charge (ζ-potential = +34.4) unlike the Ph-CS-mPEG (ζ-potential = -50 mV) [28] implying the

positive charges introduced by HTAP group with %DS of 73.3 ± 3.1% was certainly enough to overcome the negative charges of the carboxylate ion dissociated from carboxyl group (pKa 4.4) which was hydrolyzed from cyclic anhydride of *O*-phthaloylchitosan that was formed as a consequence of phthaloyl substitution at hydroxyl position.

In contrast, a nanometer-sized range (0.13±0.01 μm) can be achieved in the case of Ph-CS-DDAMT of which hydrophilic quaternary ammonium entity contains a long chain decyl group. It is believed that this group should somewhat facilitate self assembly process by providing steric stabilization similar to mPEG. The relatively low degree of DDAMT substitution (16.8 ± 0.2 %) was, however, not enough to overcome the negative charge from carboxylate ion due to the *O*-phthaloyl substitution. Therefore, the particle charge fell into the negative range.

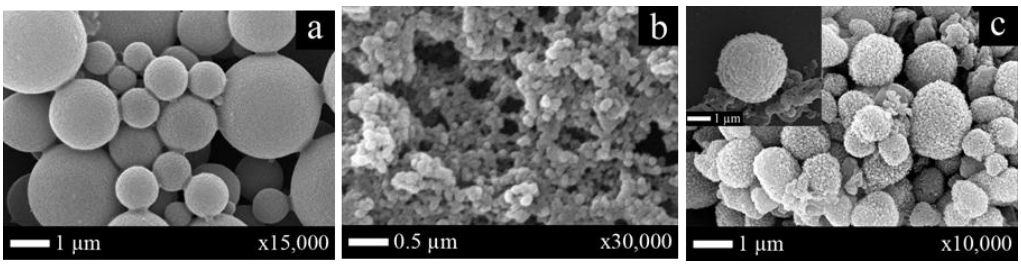

Figure 4.10 SEM micrographs of amphiphilic chitosan particles: (a) Ph-CS-HTAP, (b) Ph-CS-DDAMT, and (c) Pyr-CS-HTAP.

Table 4.1 Particle size and charge density of amphiphilic chitosan particles

Sample	$\%DS_{hydrophobic}$	$\%DS_{hydrophilic}$	Size (μm)	ζ-potential (mV)
Ph-CS-HTAP	128.8 ± 1.8	73.3 ± 3.1	1.50±0.69	+34.4
Ph-CS-DDAMT	128.8 ± 1.8	16.8 ± 0.2	0.13±0.01	-23.2
Pyr-CS-HTAP	61.1 ± 0.6	48.8 ± 0.2	1.17±0.46	+49.4

Surprisingly, it has been discovered that Pyr-CS-HTAP exhibited a unique blackberry-like morphology with a size range of 1.17±0.46 μm. To the best of our knowledge, such a morphological feature has never been reported before for organic-based materials. The most relevant work was reported in 2007 by Andreozzi *et al.*

[48] on the organic-inorganic hybrid particles fabricated from silica nanoparticles hydrophobized with octadecanol (HM) and adsorbed with copolymer of pullulan-*grafted*-poly(methyl methacrylate). The surface coverage density of these particles can be controlled by the mole ratios between the grafted copolymer and the HM nanoparticles and solvent property. It was found that the mixing components in DMF and adding water in continuous elution gradient, led to uniformly polymer-grafted nanoparticles and to blackberry-like particles under saturation conditions. In such system, the polar groups in the polymer chains face outward from the particles and give rise to corrugations on their surface. Unlike the work reported by Andreozzi *et al.*, our blackberry-like particles were formulated in one step without the need of core material.

According to TEM micrographs shown in Figure 4.11a, it seems that each individual particle consists of aggregated nanoparticles which were separated in the media used for bacteria culture of which their cross section after fixing with glutaraldehyde solution can be seen in Figure 4.11b. Only particles having positive charges, namely Ph-CS-HTAP and Pyr-CS-HTAP were subjected to the tests for antibacterial activity.

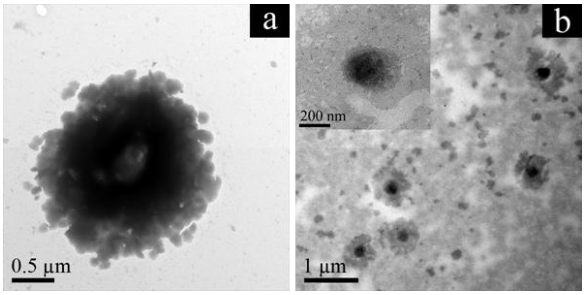

Figure 4.11 TEM micrographs of (a) Pyr-CS-HTAP particles and (b) their cross section in bacteria culture media after fixing with glutaraldehyde solution.

4.4.2 Stability of Pyr-CS-HTAP Particles

To study the stability of Pyr-CS-HTAP particles, they were dispersed under various conditions. The SEM images of the particles under those circumstances are illustrated in Figure 4.12. It was found that the self-assembled Pyr-CS-HTAP particles are relatively stable considering that there was not significant morphological change

under extreme variation of pH (from 1 to 12) and temperature (from 0 to 100^{o}C). The particles remained in blackberry-like form, but with smoother surface at 0^{o}C (Figure 4.12e). A certain extent of de-aggregation took place when treated with ethanol (EtOH), a less polar solvent than water (Figure 4.12i). The complete de-aggregation of the particles only occurred upon the treatment with non-polar hexane (Figure 4.12k). Nonetheless, the blackberry-like particles can be recovered after EtOH or hexane removal and water replacement (Figure 4.12j and l) indicating that the self-assembly process is reversible.

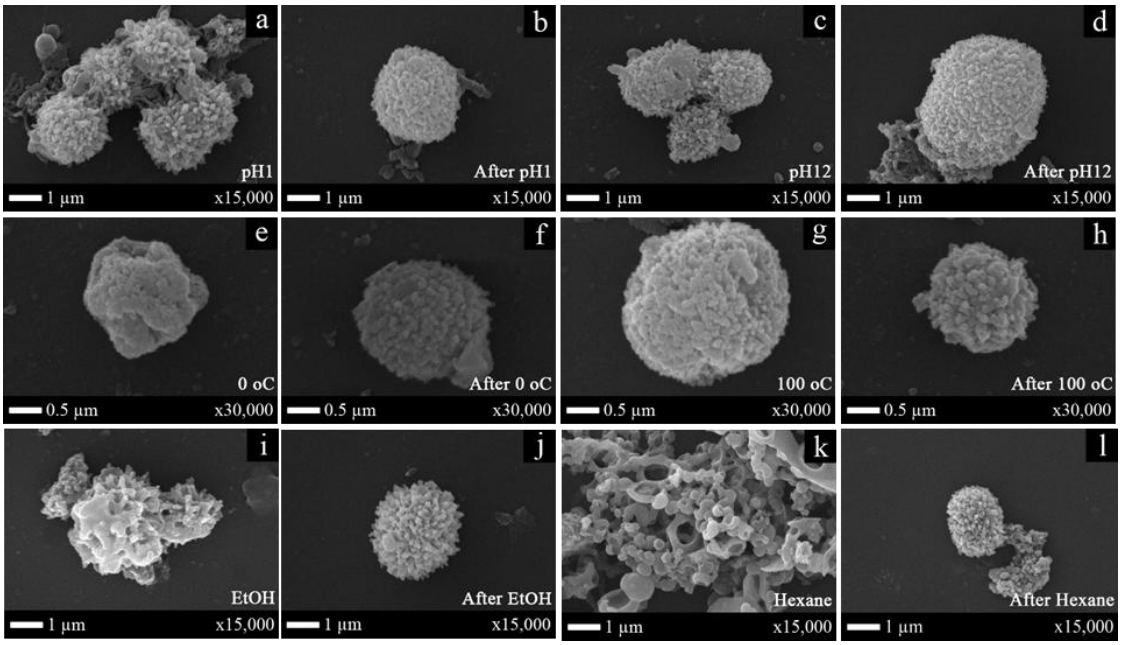

Figure 4.12 SEM micrographs of Pyr-CS-HTAP particles under various conditions: (a) pH 1, (b) after pH 1, (c) pH 12, (d) after pH 12, (e) 0^{o}C, (f) after 0^{o}C, (g) 100^{o}C, (h) after 100^{o}C, (i) EtOH, (j) after EtOH, (k) hexane, and (l) after hexane.

4.4.3 Fluorescent Property of Pyr-CS-HTAP and Dye-encapsulated Ph-CS-HTAP Particles

The bright green fluorescence of the particles appeared in Figure 4.13a indicated the existence of pyrene-tagged in the structure of Pyr-CS-HTAP particles. It should be emphasized that the fluorescence intensity would not bleach and remained almost unchanged by repetitive excitation during observation under fluorescence microscope suggesting the benefit of having fluorescence labeling done by covalent

attachment. Also, the fluorescence emission was not affected by the extreme variation of pH and temperature as mentioned above (images not shown).

In the case of the Ph-CS-HTAP particles, dye encapsulation was necessary to introduce fluorescent molecules to the particles which can be used for further investigation on antibacterial activity by fluorescence technique. Figure 4.13b and c display the red and green fluorescence emission from the Ph-CS-HTAP particles encapsulated with nile red (26.40%encapsulation) and pyrene (12.07%encapsulation), respectively. It is important to note that the fluorescence micrographs of encapsulated particles were taken after the particles were rinsed thoroughly with acetone to eliminate the left over dyes from encapsulation.

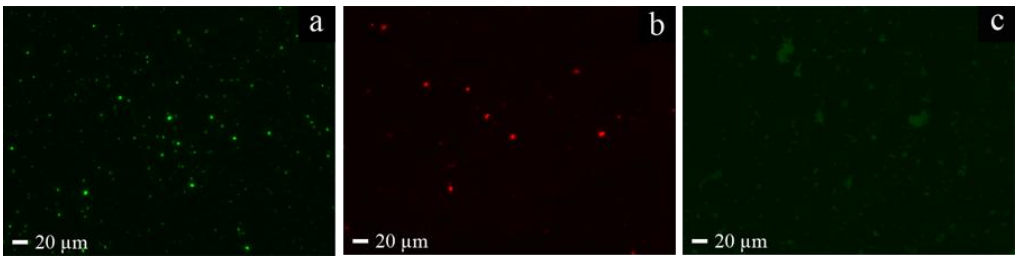

Figure 4.13 Fluorescence micrographs of (a) Pyr-CS-HTAP and Ph-CS-HTAP after nile red (b) and pyrene (c) encapsulation.

4.5 Antibacterial Activity of Amphiphilic Chitosan Particles

To test the antibacterial activity of amphiphilic chitosan particles, broth solution was used as a negative control. Broth solution with ampicillin (50 mg/mL) was used as positive control for the antibacterial tests against *S. aureus* and *E. coli* and that with tetracycline (200 µg/mL) was used as a positive control for the antibacterial test against *E. coli HB101 pGLO*. The colonies of viable bacteria were counted after being spread on agar plate and incubated for 18 h. The results are expressed as viable count (CFU/mL) value. It should be noted that *E. coli HB101 pGLO* is fluorescent-tagged bacteria that can show bright green fluorescence emission as determined by fluorescence microscope.

From Table 4.2, it is obvious that none of the amphiphilic particles exhibit antibacterial activity against all three bacterial strains tested as can be realized from the number of viable counts being almost unchanged suggesting that their growth

were normal and not interfered by the presence of particles. The ineffective antibacterial activity was later confirmed by SEM analysis. The morphology of rod-like *E.coli HB101 pGLO* were not at all affected by the two particles tested: nile red-encapsulated Ph-CS-HTAP and Pyr-CS-HTAP (Figure 4.14b-c) when compared with that of the native one (Figure 4.14a). Nonetheless, the particles can somewhat infiltrated inside the bacterial cells and caused some cell breakage as can be observed from the cross-sectional TEM images (Figure 4.14e-f). This invasion, somehow, was not detrimental enough to have measurable impact on the bacterial growth.

Table 4.2 Viable cell counts of bacteria after being treated with amphiphilic chitosan particles

Sample	Viable cell counts (Log(CFU/mL)[a]		
	S.aureus	***E.coli***	***E.coli HB101 pGLO***
Control	7.38 ± 0.06	7.93 ± 0.10	7.18 ± 0.24
Ph-CS-HTAP	7.42 ± 0.07	-	7.38 ± 0.02
Pyrene-encapsulated Ph-CS-HTAP	-	-	7.10 ± 0.15
Nile red-encapsulated Ph-CS-HTAP	-	-	7.12 ± 0.06
Pyr-CS-HTAP	-	7.87 ± 0.10	-

[a] The symbol "-" indicates that the experiment was not performed.

Further investigation on antibacterial activity against *E. coli HB101 pGLO* was performed using CLSM. In Figure 4.15, the merged images of the nile red-encapsulated Ph-CS-HTAP particles were separated by applying GFP and nile red channels which indicated the fluorescence signal from the bacteria and the particles, respectively. In the case of Pyr-CS-HTAP particles, the image of DIC mode (differential interference contrast) was superimposed on the same position of green fluorescence image of Pyr-CS-HTAP particles. Due to the highly aggregated nature of the particles, we are unable to identify whether the particles can penetrate inside the bacterial cells or just covered the outside of bacteria.

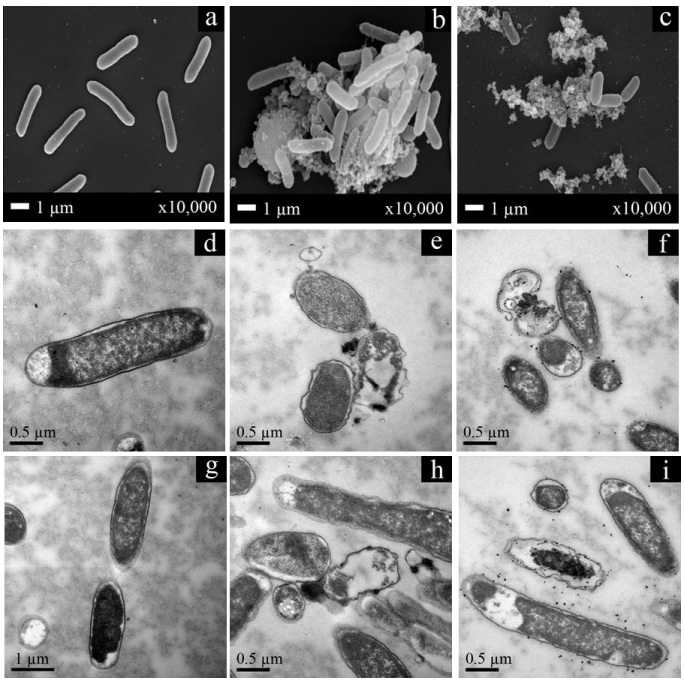

Figure 4.14 SEM (a-c) and cross-sectional TEM (d-i) micrographs of *E. coli HB101 pGLO* before (a,d,g) and after incubated with amphiphilic chitosan particles (0.5 mg/mL) for 24 h: nile red-encapsulated Ph-CS-HTAP particles (b,e,h), and Pyr-CS-HTAP particles (c,f,i).

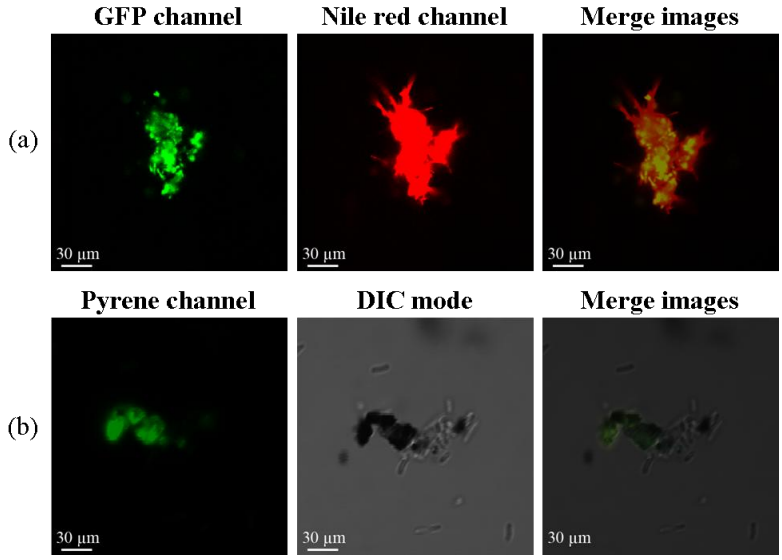

Figure 4.15 Confocal fluorescence images of *E. coli HB101 pGLO* after incubated with amphiphilic chitosan particles (0.5 mg/mL) for 24 h: (a) nile red-encapsulated Ph-CS-HTAP and (b) Pyr-CS-HTAP particles. Scale bar = 30 µm at magnification of 100x.

4.6 Cytotoxicity and Cellular Uptake of Pyr-CS-HTAP Particles

The cytotoxicity of Pyr-CS-HTAP particles was tested with mouse leukaemic monocyte macrophage cell line (RAW 264.7 cells) using MTT assay. In principle, MTT compound can be reduced to purple formazan in living cells by the mitochondrial reductase enzyme (Scheme 4.9). Thus, the more concentration of formazan determined by UV-VIS technique, the more viability of RAW 264.7 cells was expressed. The viability of RAW 264.7 cells in the presence of Pyr-CS-HTAP particles is shown in Figure 4.16. The cell viability seems to be concentration dependent up to 20 μg/mL suggesting that they are non-toxic to RAW 264.7 cells.

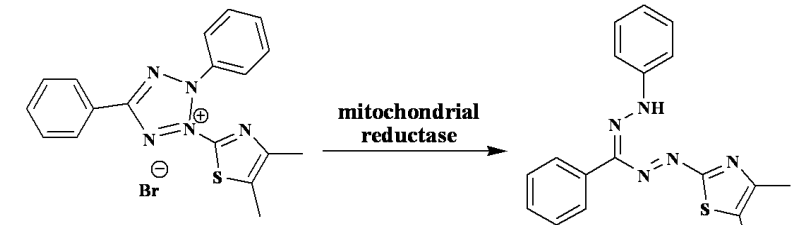

Scheme 4.9 Reduction of MTT compound by mitochondrial reductase to yellow formazan compound

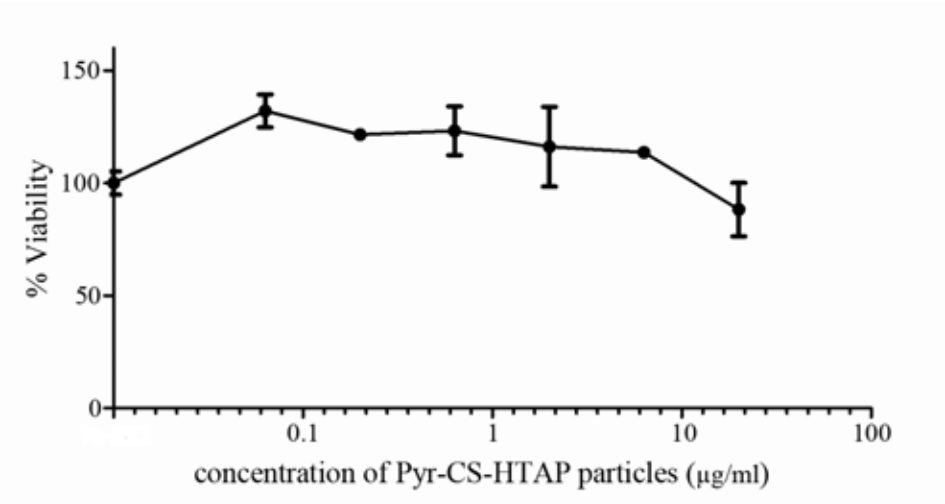

Figure 4.16 Viability of RAW 264.7 cells after being treated with varied concentration of Pyr-CS-HTAP particles (μg/mL) for 24 h.

Cellular uptake of Pyr-CS-HTAP particles by RAW 264.7 cells was monitored by CLSM technique as shown in Figure 4.17. The cells were stained with fluorescence dye, DAPI that appear in blue. The particles, on the other hand, appear both in green and red (See pyrene channel). These two emission spectra of pyrene (Figure 4.18) can be explained as a result of different degree of aggregation. It was found that the more aggregated particles, the more red shift of emission spectrum was observed. [49] In our case, it was found that the non-aggregated particles, presumably having nanometer size and green fluorescence emission, can penetrate inside the nuclei. In contrast, the aggregated particles, having red fluorescence emission, can only be taken into cytoplasm of RAW 264.7 cells. This indicated that the particle size is an important factor determining the ability to be taken by the cells.

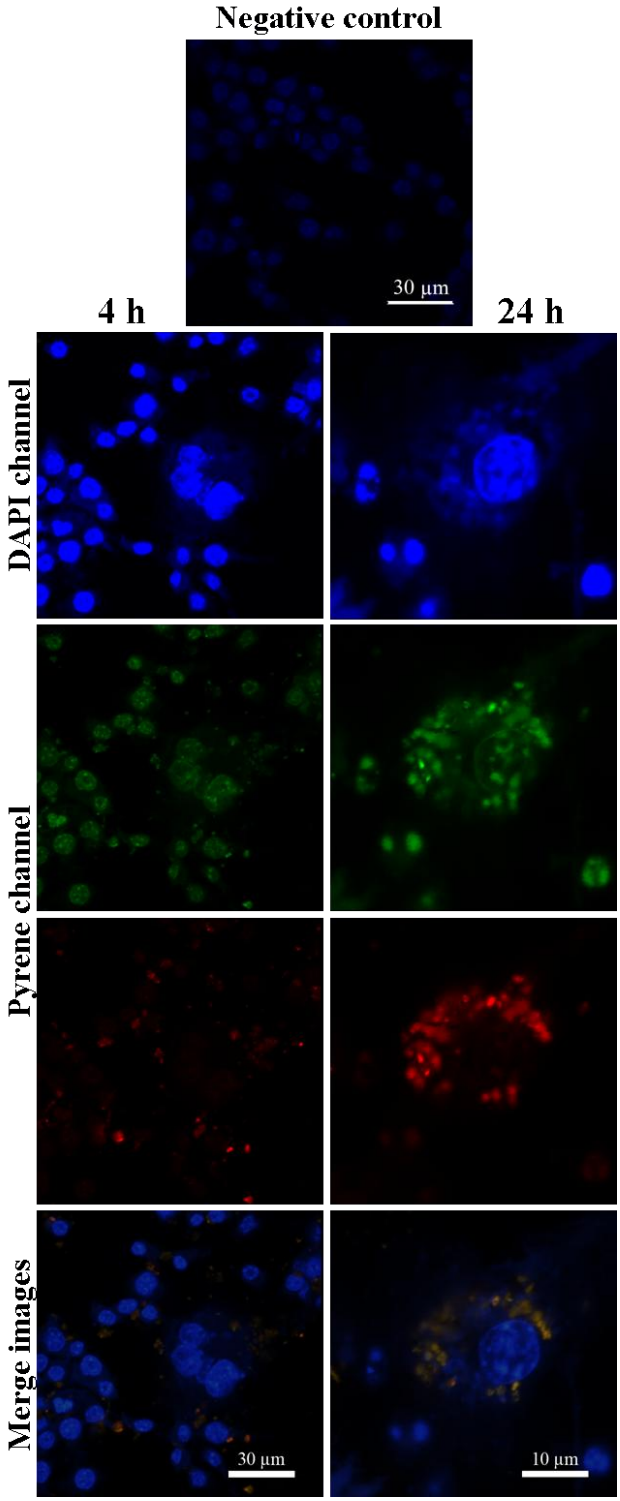

Figure 4.17 Confocal fluorescence images of cellular uptake of Pyr-CS-HTAP into RAW 264.7 cells. Cells treated with particles for 4 h (left column) and 24 h (right column). Scale bar = 30 µm at magnification 100x.

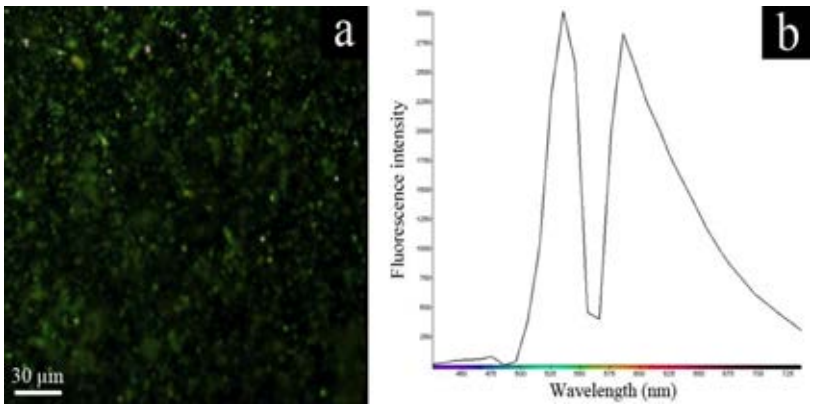

Figure 4.18 Confocal fluorescence image (a) and emission spectrum (b) of Pyr-CS-HTAP particles (solid). Scale bar = 30 µm at magnification 100x.

The Pyr-CS-HTAP particles were found to be able to encapsulate, a model hydrophobic molecule, nile red with %encapsulation efficiency of 16.20%. After encapsulation, the blackberry-like particles showed orange fluorescence emission owing to the superimposition of 2 fluorescence emission (green fluorescence of pyrene and red fluorescence of nile red) (Figure 4.19)

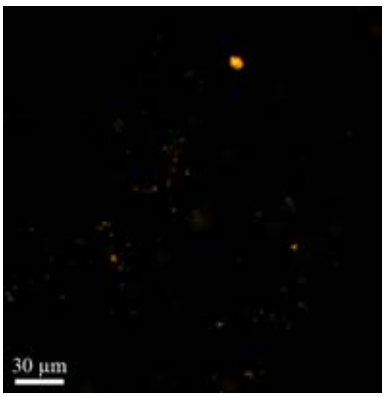

Figure 4.19 Confocal fluorescence image of Pyr-CS-HTAP particles (solid) after nile red encapsulation. Scale bar = 30 µm at magnification 100 x.

Although the developed fluorescently labeled amphiphilic chitosan particles, Pyr-CS-HTAP do not express antibacterial activity, the preliminary results on cytocompatibility, the ability to be taken up by cells and encapsulate the dye suggest that these particles are potential material for controlled delivery and bioimaging applications.

CHAPTER V
CONCLUSIONS AND SUGGESTIONS

Three types of amphiphilic chitosan were successfully synthesized from phthaloylchitosan (PhCS) formerly prepared by ring opening of phthalic anhydride by chitosan. The first derivative designated as Ph-CS-HTAP was prepared by attaching *N*-[(2-hydroxyl-3-trimethylammonium)]propyl (HTAP) group via ring opening of glycidyltrimethylammonium chloride (GTMAC) by hydroxyl groups of PhCS. Bromination followed by azidation of PhCS yielded azide-functionalized PhCS (N_3-PhCS) which subsequently gave the second derivative having 4-[(*N*-decyl-*N,N*-dimethylammonium methyl)]triazolyl (DDAMT) as hydrophilic entity (Ph-CS-DDAMT) upon Click reaction by 1,3-dipolar cycloaddition with *N,N*-dimethyl-*N*-prop-2-yn-1-yldecan-1-ammonium bromide**.** By clicking the N_3-PhCS with 1-ethynylpyrene, followed by deprotection of phthaloyl groups by hydrolysis and ring opening of GTMAC, the third derivative having pyrene as hydrophobic entity and HTAP as hydrophilic entity (Pyr-CS-HTAP) can be obtained. All derivatives were characterized by ^{1}H NMR and FT-IR.

Upon final purification of all derivatives by dialysis in water, spherical-like particles were formed by self-assembly process. Both Ph-CS-HTAP and Pyr-CS-HTAP particles were positively charged (ζ-potential = +34.4 and +49.4 mV, respectively) and have size in a micrometer range (1.50±0.69 and 1.17±0.46 μm, respectively). Although Ph-CS-DDAMT particles were much smaller in size (0.13±0.01 μm), they possessed negative charge (ζ-potential =-23.2 mV) which can be explained as a result of $\%DS_{DDAMT}$ being relatively low. Interestingly, Pyr-CS-HTAP particles exhibited blackberry-like morphology, the feature that has never been reported before for organic-based material. The structures were quite stable and not sensitive to temperature (0-100^{o}C) and pH (1-12) variation. The assembled particles de-aggregated upon the treatment with less polar solvents (ethanol, hexane) but can be recovered after solvent removal and water replacement.

Antibacterial activity testes were conducted on Pyr-CS-HTAP and Ph-CS-HTAP particles encapsulated with fluorescence dyes (pyrene, nile red). As evaluated

by viable cell counting, none of them exhibited activity against *E. coli* and *S. aureus* and the fluorescent-labeled *E. coli HB101 pGLO* although cross-sectional TEM analysis suggested that there were some rupture of bacterial membranes and the particle infiltrated inside the bacterial cells after incubation for 24 h.

The blackberry-like Pyr-CS-HTAP particles were found to be non-toxic to RAW 264.7 cells. As visualized by CLSM technique, the non-aggregated particles, presumably having nanometer size and green fluorescence emission, can penetrate inside the nuclei of the RAW 264.7 cells whereas the aggregated particles, having red fluorescence emission, can only be taken into cytoplasm of the cells. The ability to encapsulate a model hydrophobic molecule, nile red, suggested that the developed fluorescently labeled amphiphilic chitosan particles, Pyr-CS-HTAP, are potential material for controlled delivery and bioimaging applications.

The use of Pyr-CS-HTAP as carriers for specific drugs for controlled delivery to designated target cells is subjected for future investigation. The fact that the blackberry-like morphology resembles that of virus cell lead to the possibility to employ the particles for non-viral gene delivery. The preparation of Ph-CS-DDAMT particles with greater $\%DS_{DDAMT}$ will also be explored. It is anticipated that the well-controlled nanosized particles may also be useful for the development of positively charged particles for drug delivery applications.

REFERENCES

[1] Kumar, M., Muzzarelli, R.A.A., Muzzarelli, C., Sashiwa, H., and Domb, A.J. Chitosan chemistry and pharmaceutical perspectives. Chemical Reviews 104 (2004) : 6017-6084.

[2] Kumar, M.A. review of chitin and chitosan applications. Reactive & Functional Polymers 46 (2000) : 1-27.

[3] Prashanth, K.V.H., and Tharanathan, R.N. Chitin/chitosan: modifications and their unlimited application potential - an overview. Trends in Food Science & Technology 18 (2007) : 117-131.

[4] Domard, A., Rinuado, M., and Terrassin, C. New method for the quaternization of chitosan. International Journal of Biological Macromolecules 8 (1986) : 105-107.

[5] Li, Z., Zhuang, X.P., Liu, X.F., Guan, Y.L., and Yao, K.D. Study on antibacterial O-carboxymethylated chitosan/cellulose blend film from LiCl/N, N-dimethylacetamide solution. Polymer 43 (2002) : 1541-1547.

[6] Gupta, D., and Haile, A. Multifunctional properties of cotton fabric treated with chitosan and carboxymethyl chitosan. Carbohydrate Polymers 69 (2007) : 164-171.

[7] Xie, Y.J., Liu, X.F., and Chen, Q. Synthesis and characterization of water-soluble chitosan derivate and its antibacterial activity. Carbohydrate Polymers 69 (2007) : 142-147.

[8] Jung, B.O., Kim, C.H., Choi, K.S., Lee, Y.M., and Kim, J.J. Preparation of amphiphilic chitosan and their antimicrobial activities. Journal of Applied Polymer Science 72 (1999) : 1713-1719.

[9] Hu, Y., Du, Y.M., Yang, J.H., Kennedy, J.F., Wang, X.H., and Wang, L.S. Synthesis, characterization and antibacterial activity of guanidinylated chitosan. Carbohydrate Polymers 67 (2007) : 66-72.

[10] Xing, K., and others. Antibacterial activity of oleoyl-chitosan nanoparticles: A novel antibacterial dispersion system. Carbohydrate Polymers 74 (2008) : 114-120.

[11] Kim, C.H., Choi, J.W., Chun, H.J., and Choi, K.S. Synthesis of chitosan derivatives with quaternary ammonium salt and their antibacterial activity. Polymer Bulletin 38 (1997) : 387-393.

[12] Seong, H.S., Whang, H.S., and Ko, S.W. Synthesis of a quaternary ammonium derivative of chito-oligosaccharide as antimicrobial agent for cellulosic fibers. Journal of Applied Polymer Science 76 (2000) : 2009-2015.

[13] Jia, Z.S., Shen, D.F., and Xu, W.L. Synthesis and antibacterial activities of quaternary ammonium salt of chitosan. Carbohydrate Research 333 (2001) : 1-6.

[14] Avadi, M.R., and others. Diethylmethyl chitosan as an antimicrobial agent: Synthesis, characterization and antibacterial effects. European Polymer Journal 40 (2004) : 1355-1361.

[15] Sajomsang, W., Tantayanon, S., Tangpasuthadol, V., and Daly, W.H. Synthesis of methylated chitosan containing aromatic moieties: Chemo selectivity and effect on molecular weight. Carbohydrate Polymers 72 (2008) : 740-750.

[16] Sajomsang, W., Gonil, P., and Saesoo, S. Synthesis and antibacterial activity of methylated N-(4-N,N-dimethylaminocinnamyl) chitosan chloride. European Polymer Journal 45 (2009) : 2319-2328.

[17] Liu, H.Q., Zhao, Y.C., Cheng, S., Huang, N., and Leng, Y.X. Syntheses of novel chitosan derivative with excellent solubility, anticoagulation, and antibacterial property by chemical modification. Journal of Applied Polymer Science 124 (2012) : 2641-2648.

[18] Yin, X.Q., Chen, J.H., Yuan, W., Lin, Q., Ji, L., and Liu, F. Preparation and antibacterial activity of Schiff bases from O-carboxymethyl chitosan and para-substituted benzaldehydes. Polymer Bulletin 68 (2012) : 1215-1226.

[19] Vallapa, N., and others. Enhancing antibacterial activity of chitosan surface by heterogeneous quaternization. Carbohydrate Polymers 83 (2011) : 868-875.

[20] Qi, L.F., Xu, Z.R., Jiang, X., Hu, C.H., and Zou, X.F. Preparation and antibacterial activity of chitosan nanoparticles. Carbohydrate Research 339 (2004) : 2693-2700.

[21] Ye, W.J., Leung, M.F., Xin, J., Kwong, T.L., Lee, D.K.L., and Li, P. Novel core-shell particles with poly(n-butyl acrylate) cores and chitosan shells as an antibacterial coating for textiles. Polymer 46 (2005) : 10538-10543.

[22] Shi, Z.L., Neoh, K.G., Kang, E.T., and Wang, W. Antibacterial and mechanical properties of bone cement impregnated with chitosan nanoparticles. Biomaterials 27 (2006) : 2440-2449.

[23] Qi, L.F., Xu, Z.R., Jiang, X., Li, Y., and Wang, M.Q. Cytotoxic activities of chitosan nanoparticles and copper-loaded nanoparticles. Bioorganic & Medicinal Chemistry Letters 15 (2005) : 1397-1399.

[24] Du, W.L., Xu, Y.L., Xu, Z.R., and Fan, C.L. Preparation, characterization and antibacterial properties against *E. coli K88* of chitosan nanoparticle loaded copper ions. Nanotechnology 19 (2008) : 5pp.

[25] Du, W.L., Niu, S.S., Xu, Y.L., Xu, Z.R., and Fan, C.L. Antibacterial activity of chitosan tripolyphosphate nanoparticles loaded with various metal ions. Carbohydrate Polymers 75 (2009) : 385-389.

[26] Wiarachai, O., Thongchul, N., Kiatkamjornwong, S., and Hoven, V.P. Surface-quaternized chitosan particles as an alternative and effective organic antibacterial material. Colloids and Surfaces B-Biointerfaces 92 (2012) : 121-129.

[27] Yoksan, R., Matsusaki, M., Akashi, M., and Chirachanchai, S. Controlled hydrophobic/hydrophilic chitosan: colloidal phenomena and nanosphere formation. Colloid and Polymer Science 282 (2004) : 337-342.

[28] Choochottiros, C., Yoksan, R., and Chirachanchai, S. Amphiphilic chitosan nanospheres: Factors to control nanosphere formation and its consequent pH responsive performance. Polymer 50 (2009) : 1877-1886.

[29] Opanasopit, P., Ngawhirunpat, T., Rojanarata, T., Choochottiros, C., and Chirachanchai, S. Camptothecin-incorporating N-phthaloylchitosan-g-mPEG self-assembly micellar system: Effect of degree of deacetylation. Colloids and Surfaces B-Biointerfaces 60 (2007) : 117-124.

[30] Kim, K., Kwon, S., Park, J.H., Chung, H., Jeong, S.Y., and Kwon, I.C. Physicochemical characterizations of self-assembled nanoparticles of glycol chitosan-deoxycholic acid conjugates. Biomacromolecules 6 (2005) : 1154-1158.

[31] Anumansirikul, N., Wittayasuporn, M., Klinubol, P., Tachaprutinun, A., and Wanichwecharungruang, S.P. UV-screening chitosan nanocontainers: increasing the photostability of encapsulated materials and controlled release. Nanotechnology 19 (2008) : 9pp.

[32] Liu, L., Xu, X., Guo, S., and Han, W. Synthesis and self-assembly of chitosan-based copolymer with a pair of hydrophobic/hydrophilic grafts of polycaprolactone and poly(ethylene glycol). Carbohydrate Polymers 75 (2009) : 401-407.

[33] Ngawhirunpat, T., and others. Incorporation methods for cholic acid chitosan-g-mPEG self-assembly micellar system containing camptothecin. Colloids and Surfaces B-Biointerfaces 74 (2009) : 253-259.

[34] Xing, K., Chen, X.G., Liu, C.S., Cha, D.S., and Park, H.J. Oleoyl-chitosan nanoparticles inhibits Escherichia coli and Staphylococcus aureus by damaging the cell membrane and putative binding to extracellular or intracellular targets. International Journal of Food Microbiology 132 (2009) : 127-133.

[35] Talaro, K.P. Foundations in microbiology. New York : McGraw-Hill, 2005.

[36] Cuero, R.G., Osuji, G., and Washington, A. N-carboxymethylchitosan inhibition of aflatoxin production: role of Zinc. Biotechnology Letters 13 (1991) : 441-444.

[37] Tsai, G.J., and Su, W.H. Antibacterial activity of shrimp chitosan against Escherichia coli. Journal of Food Protection 62 (1999) : 239-243.

[38] Shahidi, F., Arachchi, J.K.V., and Jeon, Y.J. Food applications of chitin and chitosans. Trends in Food Science & Technology 10 (1999) : 37-51.

[39] Rabea, E.I., Badawy, M.E.T., Stevens, C.V., Smagghe, G., and Steurbaut, W. Chitosan as antimicrobial agent: Applications and mode of action. Biomacromolecules 4 (2003) : 1457-1465.

[40] Raafat, D., von Bargen, K., Haas, A., and Sahl, H.G. Insights into the mode of action of chitosan as an antibacterial compound. Applied and Environmental Microbiology 74 (2008) : 3764-3773.

[41] Kolb, H.C., Finn, M.G., and Sharpless, K.B. Click chemistry: Diverse chemical function from a few good reactions. Angewandte Chemie-International Edition 40 (2001) : 2004-2012.

[42] Tornoe, C.W., Christensen, C., and Meldal, M. Peptidotriazoles on solid phase: 1,2,3-triazoles by regiospecific copper(I)-catalyzed 1,3-dipolar cycloadditions of terminal alkynes to azides. Journal of Organic Chemistry 67 (2002) : 3057-3064.

[43] Hvilsted, S. Facile design of biomaterials by 'click' chemistry. Polymer International 61 (2012) : 485-494.

[44] Gao, Y., Zhang, Z.W., Chen, L.L., Gu, W.W., and Li, Y.P. Synthesis of 6-N,N,N-Trimethyltriazole Chitosan via "Click Chemistry" and Evaluation for Gene Delivery. Biomacromolecules 10 (2009) : 2175-2182.

[45] Zampano, G., Bertoldo, M., and Ciardelli, F. Defined Chitosan-based networks by C-6-Azide-alkyne "click" reaction. Reactive & Functional Polymers 70 (2010) : 272-281.

[46] Riva, R., Lussis, P., Lenoir, S., Jerome, C., Jerome, R., and Lecomte, P. Contribution of "click chemistry" to the synthesis of antimicrobial aliphatic copolyester. Polymer 49 (2008) : 2023-2028.

[47] Aranaz, I., Harris, R., and Heras, A. Chitosan Amphiphilic Derivatives. Chemistry and Applications. Current Organic Chemistry 14 (2010) : 308-330.

[48] Andreozzi, P., Mesa, C., Masci, G., and Suber, L. Formation and physicochemical characterization of silica-based blackberry-like nanoparticles capped by polysaccharides. Journal of Physical Chemistry C 111 (2007) : 18004-18009.

[49] Wang, Z.Q., Xu, C., Wang, W., Dong, X., Zhao, B., and Ji, B. Novel pyrene derivatives: Synthesis, properties and highly efficient non-doped deep-blue electroluminescent device. Dyes and Pigments 92 (2011) : 732-736.

APPENDIX

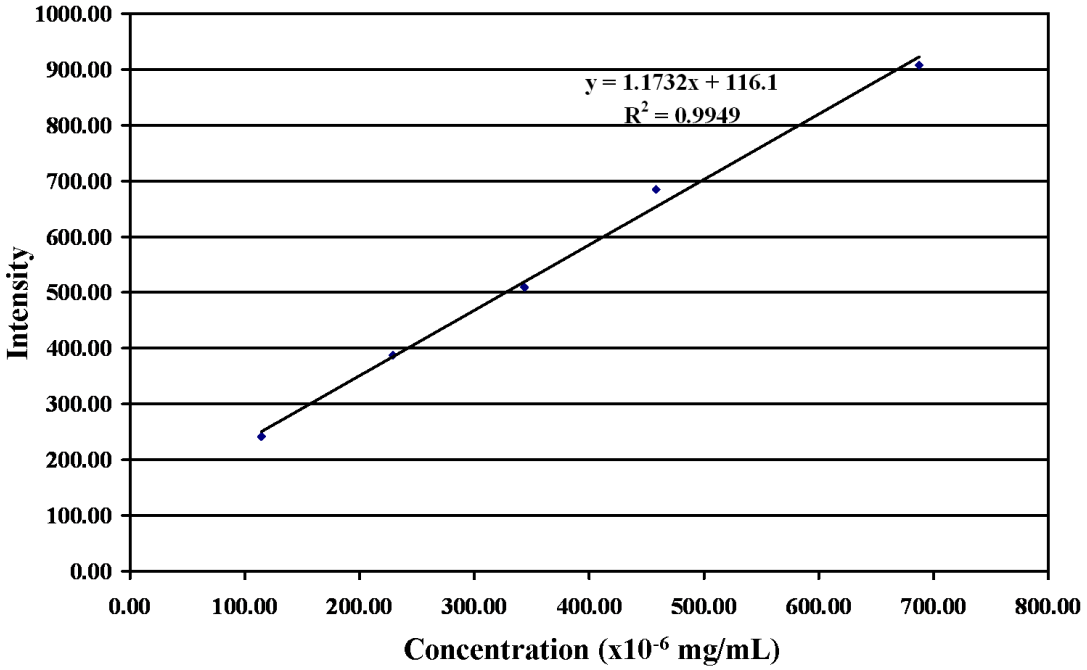

Figure A-1 Standard curve of fluorescence intensity at wavelength 393 nm as a function of pyrene concentration of ($x10^{-6}$ mg/mL).

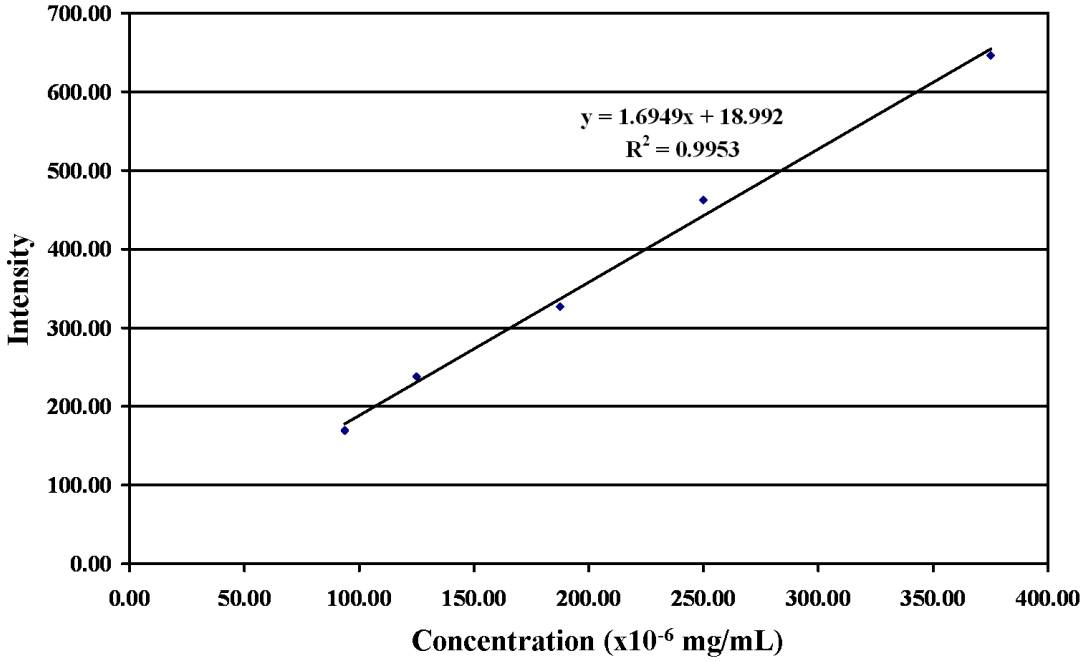

Figure A-2 Standard curve of fluorescence intensity at wavelength 607 nm as a function of nile red concentration of ($x10^{-6}$ mg/mL).

Table A-1 Data of the intensity and concentration of pyrene and nile red in the encapsulated particles.

Particles	Intensity of 393 nm	$[C]_{pyrene}$ ($x10^{-6}$mg/mL)	$\%EE_{pyrene}$	Intensity of 607 nm	$[C]_{nile\ red}$ ($x10^{-6}$mg/mL)	$\%EE_{nile\ red}$
Ph-CS-HTAP 129:73	682.90	483.12	12.07	293.15	161.75	26.40
Pyr-CS-HTAP 61:49	-[a]	-[a]	-[a]	539.23	306.94	16.20

[a] The experiment using this particle was not performed.

Example Calculation of total amount of encapsulated pyrene in Ph-CS-HTAP particles.

The pyrene-encapsulated Ph-CS-HTAP particles showed the intensity of pyrene at 393 nm of 682.90.

The linear equation of standard curve in Figure A-3 is;

$$y = 1.1732x + 116.1$$

If the intensity (y) is 682.90, the concentration (x) after twice dilution will be;

$$682.90 = (1.1732) \times (x) + 116.1$$

$$x = 483.12 \times 10^{-6} \text{ mg/mL}$$

The second dilution;

$$N_2V_2 = N_3V_3$$

$$N_2 \times (1500\ \mu L) = (483.12 \times 10^{-6} \text{ mg/mL}) \times (3000\ \mu L)$$

$$N_2 = 966.24 \times 10^{-6} \text{ mg/mL}$$

The first dilution;

$$N_1V_1 = N_2V_2$$

$$N_1 \times (30\ \mu L) = (966.24 \times 10^{-6} \text{ mg/mL}) \times (2730\ \mu L)$$

$$N_1 = 0.0879 \text{ mg/mL}$$

The amount of pyrene (mg) in 30 μL;

$$g = (0.0879 \text{ mg}/1000\ \mu L) \times (30\ \mu L)$$

$$g = 0.0026 \text{ mg}$$

The amount of pyrene (mg) in 50 mL;

$$g = (0.0026 \text{ mg}/30\ \mu L) \times (50{,}000\ \mu L)$$

$$g = 4.3964 \text{ mg}$$

Then, the %encapsulation efficiency (%EE) of pyrene in Ph-CS-HTAP particles can be calculated by the following equation;

$$\%Encapsulation\ Efficiency = \left\{ \frac{\text{initial amount of dye (mg) - left over amount of dye (mg)}}{\text{initial amount of dye (mg)}} \right\} \text{x } 100$$

With the initial amount of pyrene of 5 mg, the %EE can be expressed as;

$$\%Encapsulation\ Efficiency = \left\{ \frac{(5\text{ mg}) - (4.3964\text{ mg})}{(5\text{ mg})} \right\} \text{x } 100$$

$$\%Encapsulation\ Efficiency = 12.07\%$$

VITAE

Miss Kanya Taboonpong was born in Ratchaburi, Thailand, on September 20th, 1986. She received a Bachelor Degree of Science (Chemistry) from the Department of Chemistry, Faculty of Science, Kasetsart University, Bangkok in 2009. In the same year, she started as a Master Degree student with a major in Program of Petrochemistry and Polymer Science, Faculty of Science, Chulalongkorn University and completed the program in 2012.

Proceedindings:

October 2011	Oral presentation in The 2nd Polymer Conference of Thailand (PCT-2), Chulabhorn Research Institute, Bangkok, Thailand. The Second Runner Up Oral Presentation Award

Presentation in Conference:

December 2011	Poster presentation in the Yearly Meeting for Research Team Consolidation Grant, The Thailand Research Fund and Fund-Higher Education Commission (RTA5280002).
January 2012	Oral presentation in Pure and Applied Chemistry International Conference (PACCON2012). Empress Hotel, Chiang Mai, Thailand. The Best Oral Presentation Session: Chemistry for Materials and Nanotechnology